SOLON: Communication-efficient Byzantine-resilient Distributed Training via Redundant Gradients

Lingjiao Chen¹, Leshang Chen², Hongyi Wang³*, Susan Davidson², Edgar Dobriban²

Stanford University¹, University of Pennsylvania², University of Wisconsin³

Abstract

There has been a growing need to provide Byzantine-resilience in distributed model training. Existing robust distributed learning algorithms focus on developing sophisticated robust aggregators at the parameter servers, but pay less attention to balancing the communication cost and robustness. In this paper, we propose SOLON, an algorithmic framework that exploits gradient redundancy to provide communication efficiency and Byzantine robustness simultaneously. Our theoretical analysis shows a fundamental trade-off among computational load, communication cost, and Byzantine robustness. We also develop a concrete algorithm to achieve the optimal trade-off, borrowing ideas from coding theory and sparse recovery. Empirical experiments on various datasets demonstrate that SOLON provides significant speedups over existing methods to achieve the same accuracy, *e.g.*, over 10× faster than BULYAN and 80% faster than DRACO. We also show that carefully designed Byzantine attacks break SIGNUM and BULYAN, but do not affect the successful convergence of SOLON.

1 Introduction

The growing size of datasets and machine learning models has led to many developments in distributed training using stochastic optimization [16, 15, 45, 13, 17]. One of the most widely used settings is the *parameter server (PS) model* [36, 34, 27], where the gradient computation is partitioned among all compute nodes, typically using stochastic gradient descent (SGD) or its variants. A central parameter server then aggregates the calculated gradients from all compute nodes to update the global model.

However, scaling PS models to large clusters introduces two challenges: guarding against *Byzantine attacks* and managing *communication overhead*. Byzantine attacks include erroneous gradients sent from unreliable compute nodes due to power outages, hardware or software errors, as well as malicious attacks. The communication overhead of sending gradients to the PS in large clusters can also be extremely high, potentially dominating the training time, [13, 3, 55, 54, 7], since the number of gradients sent is linear in the number of compute nodes.

Although recent work has studied the problem of Byzantine attacks under the PS model [4, 23, 56], the communication overhead remains prohibitive. For example, [6, 10, 59, 12] use *robust aggregators* at the PS to mitigate unreliable gradients, while [7] introduces *algorithmic redundancy* to detect and remove Byzantine nodes. Robust aggregators are computationally expensive due to their super-linear (often quadratic) dependence on the number of nodes. They also often have limited convergence guarantees under Byzantine attacks, e.g., only establishing convergence in the limit, or only guaranteeing that the output of the aggregator has a positive inner product with the true gradient. They often require strong bounds on the dimension of the model. Although algorithmic redundancy or coding-theoretic [50, 7] approaches offer strong convergence guarantees, these approaches have high communication overhead.

^{*}The first three authors contributed equally to this paper.

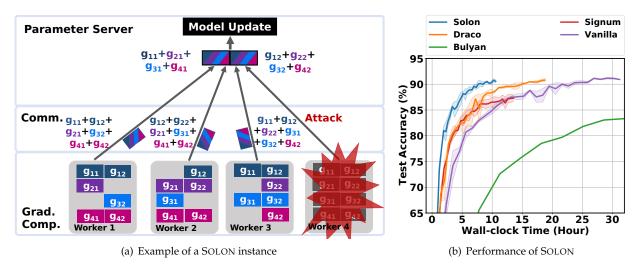


Figure 1: Demonstration of SOLON. (a) gives an example of SOLON, where the cluster consists of four compute nodes. (b) shows the runtime performance of SOLON $r_c = 10$ when training ResNet-18 on CIFAR-10 under rev-grad attack. Compared to various baselines, SOLON converges faster and provides higher final accuracy.

Thus, it remains an open question to simultaneously provide *Byzantine-resilience with strong guarantees and communication efficiency* for distributed learning.

To address this problem, we propose SOLON, a distributed training framework leveraging algorithmic redundancy to protect against Byzantine attacks, and ideas from sparse recovery [43] and coding theory [50] to reduce communication overhead. The approach is as follows: In a Byzantine-free PS model with P compute nodes and B gradients to be computed, at each iteration each of the P nodes computes B/P gradients, and sends them to the PS. In SOLON, gradients are computed redundantly to tolerate Byzantine failures; each node computes rB/P gradients, incurring a *computational redundancy ratio* of r. To reduce communication overhead, compressed gradients are sent to the PS. For d-dimensional gradients, each node only sends a d/r_c -dimensional vector to the PS, where r_c is the *compression ratio*.

We show that under worst-case adversarial conditions where the adversarial nodes have access to the complete data and gradients, and can send arbitrary results to the PS, there is a fundamental trade-off among Byzantine-resilience, communication overhead and computation cost. To tolerate s Byzantine nodes, the redundancy ratio must satisfy $r \geq 2s + r_c$. We provide a concrete encoding and decoding technique for SOLON based on Vandermonde matrices and building on Prony's method from signal processing [43, 58] that matches the optimal condition $r = 2s + r_c$.

Example. Figure 1(a) shows four two-dimensional gradient vectors, g_1, g_2, g_3, g_4 , where gradients $g_i = (g_{i1}, g_{i2})$ are in different colors. To tolerate Byzantine workers, each node computes four gradients. However, instead of sending a two-dimensional vector to the PS, each node only sends a one-dimensional linear combination of the elements in the local gradients. For instance, worker 1 computes and sends the scalar $g_{11} + g_{12} + g_{21} + g_{32} + g_{41} + g_{42}$. Here, the redundancy ratio r = 4 and the compression ratio $r_c = 2$. The PS uses a decoding scheme presented in Section 3. Therefore SOLON can recover the correct gradient with one Byzantine worker $(4 \ge 2 \times 1 + 2)$.

We implemented SOLON in Pytorch and conducted extensive experiments on a large cluster. Our results show that SOLON can provide significant speedups across various ML models and datasets over existing methods, such as BULYAN [23] and DRACO [7], shown in Figure 1(b) using ResNet-18 [24] on CIFAR-10 [31] under a reverse gradient attack. In addition, SOLON successfully defends against strong Byzantine attacks such as "A little is enough" (ALIE) [4], on which some methods such as BULYAN and SIGNUM [5] fail to converge or result in significant accuracy loss, see Section 4.

Contributions. Our contributions include:

- 1. SOLON, a distributed training framework that exploits algorithmic redundancy to simultaneously provide Byzantine-resilience and communication efficiency.
- 2. A concrete encoding and decoding mechanism, which is provably efficient and achieves the optimal trade-off between Byzantine resilience, communication overhead, and computational cost.
- 3. Extensive experiments which show that SOLON exhibits significant speedups as well as strong Byzantine-resilience over previous approaches.

The SOLON framework can be used for any distributed algorithm which requires the sum of multiple functions, including gradient descent, SVRG [28], coordinate descent, and projected or accelerated versions of these algorithms. However, in this paper, we focus on mini-batch SGD. The rest of the paper is organized as follows: Section 2 discusses related work. Section 3 presents the SOLON framework and theoretical guarantees. Experimental results are given in Section 4.

2 Related work

Byzantine fault tolerance against worst-case and/or adversarial failures such as system crashes, power outages, software bugs, and adversarial agents that exploit security flaws has been extensively studied since the 1980s [32]. In distributed machine learning, these failures may appear when a subset of compute nodes returns to the PS erroneous updates. It is well understood that first-order methods, such as gradient descent or mini-batch SGD, are not robust to Byzantine errors; even a single erroneous update can introduce arbitrary errors to the optimization variables [6, 10]. At the same time, distributed model training suffers from communication overhead due to frequent gradient updates transmitted between compute nodes [14, 38, 35, 30, 17, 18]. SOLON aims at improving both Byzantine-resilience and communication-efficiency in distributed model training.

More recently, attention has turned to Byzantine-resilient distributed machine learning techniques. Results show that while average-based gradient methods are susceptible to adversarial nodes, robust gradient aggregation methods can, in some cases, achieve better convergence while being robust to some attacks [10, 20, 6, 57, 56, 6, 59, 23, 29]. Despite theoretical guarantees, the proposed algorithms often only ensure a weak form of resilience against Byzantine failures, and can fail against strong Byzantine attacks [23, 56, 4]. Another line of work proposes to use algorithmic redundancy to attain black-box Byzantine-resilience guarantees. However, many of these techniques require redundant computation from compute nodes (such as DRACO [7]) or place a heavy computation overhead on the PS (such as BULYAN [23]). Furthermore, they introduce a heavy communication overhead. [42] interpolates between DRACO and robust aggregation methods for faster computation on both compute nodes and the PS. However, it does not mitigate the communication bottleneck, whereas SOLON introduces both black-box Byzantine-resilience guarantee and communication-efficiency.

Communication-efficient distributed machine learning has gained a lot of attention. Various methods propose to use gradient compression, *e.g.*, via quantization [44, 2, 55, 49] or sparsification [48, 54, 37, 53, 1] to enhance the communication efficiency. These methods massively compress the gradients, however, their Byzantine-resilience is not clear.

The methods that are the most similar to SOLON are SIGNUM [5] and the one proposed in [22]. These methods introduce both communication-efficiency and Byzantine-resilience, however their Byzantine-resilience guarantees are not as strong as for SOLON in theory, i.e. they typically use lossy compression for coding and decoding schemes, which only achieve approximated recovery under certain attacks. [58] considers the trade-offs between communication efficiency and straggler tolerance. On the other hand, our work focuses on improving communication efficiency in a Byzantine-aware distributed system.

3 Solon

In this section we give an overview of the SOLON framework, discuss constraints on the encoding and decoding functions, and define optimal coding schemes.

The proofs are left to the appendix.

3.1 Preliminaries

Basic notations. For a matrix \mathbf{A} , let $\mathbf{A}_{i,j}$, $\mathbf{A}_{i,\cdot}$, and $\mathbf{A}_{\cdot,j}$ denote entries, rows, and columns, respectively. More generally, $\mathbf{A}_{S,T}$ is the submatrix of \mathbf{A} with rows indexed by S and columns indexed by T. The Hadamard, or elementwise, product $\mathbf{A} \odot \mathbf{B}$ of two matrices of the same size has entries $(\mathbf{A} \odot \mathbf{B})_{i,j} = \mathbf{A}_{i,j} \mathbf{B}_{i,j}$. Let m be the dimension of the data, n be the size of the training set, and $\mathbf{x}_i \in \mathbb{R}^m$, $i=1,\ldots,m$ be the data points. Let $\ell(\cdot;\cdot)$ be the loss function, d be the model dimension, and $\mathbf{w} \in \mathbb{R}^d$ be the model parameters. Let $\mathbf{1}_m$ and $\mathbf{1}_{n \times m}$ be the $m \times 1$ vector, and $n \times m$ matrix, of all ones, respectively. Similarly, let $\mathbf{0}_m, \mathbf{0}_{n \times m}$ contain zeros. The empirical risk minimization (ERM) [51, 52] objective is: $\min_{\mathbf{w}} n^{-1} \sum_{i=1}^n \ell(\mathbf{w}; \mathbf{x}_i)$. The most common current approach is to use first-order stochastic optimization to solve this, in particular mini-batch stochastic gradient descent (SGD). Starting at an initial point \mathbf{w}_0 , we iterate $\mathbf{w}_k = \mathbf{w}_{k-1} - \gamma/|S_k| \sum_{i \in S_k} \nabla \ell_{\mathbf{w}}(\mathbf{w}_{k-1}; \mathbf{x}_i)$, where $S_k \subseteq \{1,\ldots,n\}$ is a random subset of size B and $\gamma > 0$ is the learning rate.

We relabel S_k to $\{1,\ldots,B\}$ and denote $\nabla \ell(\mathbf{w}_{k-1};\mathbf{x}_i)$ by \mathbf{g}_i .

Distributed learning. We aim to compute $\mathbf{g} = \sum_{i=1}^{B} \mathbf{g}_i$ in a distributed, adversary-resistant, and communication efficient manner. We consider a distributed training model where gradient computations are partitioned across P compute nodes at each iteration. These operate on a potentially reduced dimension d_c for communication efficiency, and we let the gradient compression ratio be $r_c \triangleq d/d_c$. After computing and summing up their assigned gradients, each node sends their answer back to the parameter server (PS). This sums them and updates the model. By applying SOLON, we reduce the communication complexity for sending gradients to server from $\mathcal{O}(Pd)$ to $\mathcal{O}(Pd_c)$. The broadcast phase of sending aggregated gradients from server to compute nodes takes $\mathcal{O}(\log{(P)d)}$, which is not the major overhead.

We assume that at most *s* compute nodes are unreliable, Byzantine, or adversarial, and can send to the PS an arbitrary update. We consider the strongest possible adversaries: with infinite computational power, knowing the entire data set, the training algorithm, any defenses present in the system, and able to collaborate.

3.2 Framework

SOLON is defined by the tuple, or *mechanism*, (\mathbf{A}, E, D) , where \mathbf{A} is an allocation matrix specifying how to assign gradients to nodes, E are encoding functions determining how each compute node should locally encode its gradients, and D is a decoding function determining how the PS should decode the output of the nodes. As an example, in Figure 1(a), A corresponds to the gradient computation assignment of the compute nodes, E corresponds to the summation of the gradients by each node, and E refers to the decoding phase at the PS. We generalize the scheme in Figure 1 to E compute nodes and E gradients.

Allocation matrix, \mathbf{A} . At each iteration of the training process, we assign the B gradients to the P compute nodes using a $P \times B$ allocation matrix \mathbf{A} , where $\mathbf{A}_{j,k}$ is equal to unity ("1") if node j is assigned to the kth gradient \mathbf{g}_k , and zero ("0") otherwise. The support of $\mathbf{A}_{j,\cdot}$, denoted supp $(\mathbf{A}_{j,\cdot})$, is the set of indices of gradients evaluated by the jth node. For simplicity, we will assume B = P. Let $\|\mathbf{A}\|_0$ be to the L_0 norm of a matrix, i.e., the number of nonzero entries. Following [7], we define the *redundancy ratio* of an allocation as the average number of gradients assigned to each compute node, or equivalently $r \triangleq \|\mathbf{A}\|_0/P$.

We define the $d \times P$ matrix \mathbf{G} with gradients as its columns: $\mathbf{G} \triangleq [\mathbf{g}_1, \mathbf{g}_2, \cdots, \mathbf{g}_P]$. The jth node first picks out its assigned gradients using the allocation matrix \mathbf{A} , computing a $d \times P$ gradient matrix $\mathbf{Y}_j \triangleq (\mathbf{1}_d \mathbf{A}_{j,\cdot}) \odot \mathbf{G}$. The columns of this matrix are \mathbf{g}_k if the kth gradient \mathbf{g}_k is allocated to the jth compute node, i.e., $\mathbf{A}_{j,k} \neq 0$, and zero otherwise.

Encoding Functions, E. The jth compute node is equipped with an encoding function E_j that maps the $d \times P$ matrix \mathbf{Y}_j of its assigned gradients to a d_c -dimensional vector. The jth compute node computes and sends $\mathbf{z}_j \triangleq E_j(\mathbf{Y}_j)$ to the PS. If the jth node is adversarial, then it instead sends $\mathbf{z}_j + \mathbf{n}_j$ to the PS, where \mathbf{n}_j is an arbitrary d_c -dimensional Byzantine vector. We let $E = \{E_1, E_2, \cdots, E_P\}$ be the set of local encoding functions.

Decoding Function, D. The $d_c \times P$ matrix $\mathbf{Z} = \mathbf{Z}^{\mathbf{A}, E, \mathbf{G}} \triangleq [\mathbf{z}_1, \mathbf{z}_2, \cdots, \mathbf{z}_P]$ contains all outputs of the nodes. The $d_c \times P$ matrix $\mathbf{N} \triangleq [\mathbf{n}_1, \mathbf{n}_2, \cdots, \mathbf{n}_P]$ contains all Byzantine vectors, with at most s non-zero columns. Then, the PS receives a $d_c \times P$ matrix $\mathbf{R} \triangleq \mathbf{Z} + \mathbf{N}$, and computes a d-dimensional vector $\mathbf{u} \triangleq D(\mathbf{R})$ using a decoding function D.

We require that the algorithm at the PS recovers the *d*-dimensional sum of gradients, G1_P:

Definition 1. SOLON with (\mathbf{A}, E, D) can tolerate s adversarial nodes, if for any $\mathbf{N} = [\mathbf{n}_1, \mathbf{n}_2, \cdots, \mathbf{n}_P]$ such that $|\{j : \mathbf{n}_i \neq 0\}| \leq s$, we have $D(\mathbf{Z} + \mathbf{N}) = \mathbf{G}\mathbf{1}_P$.

If we defend against the Byzantine attack, then the model update at each iteration is identical to the adversary-free setting. This implies that convergence guarantees for the adversary-free case transfer to the adversarial case.

3.3 Encoding and decoding functions

What are the fundamental limits of the above allocation, encoding, and decoding schemes, in particular of the redundancy ratio used in allocation and the compression ratio used in encoding? Perhaps surprisingly, the redundancy ratio does not depend on the compression ratio. The encoded gradients at each compute node can be arbitrarily compressed without affecting the our ability to tolerate Byzantine attacks. The reason is that any *d*-dimensional real vector can be mapped one-to-one to a real number. This is stated in the following theorem.

Theorem 1. If there is a mechanism (\mathbf{A}, E, D) of gradient allocation, encoding, and decoding with redundancy ratio r tolerating s adversarial nodes with a compression ratio r_c of unity, then there is a mechanism (\mathbf{A}', E', D') with redundancy ratio r tolerating s adversarial nodes for any compression ratio $r_c > 0$.

However (\mathbf{A}', E', D') is in a sense pathological and it is unclear if it can reduce the the number of bits communicated. Therefore, we seek classes of *regular* encoder and decoder functions E, D, to reduce communication cost.

Definition 2. A set of encoding functions E is called regular if each output element of each function E_j is a function of linear combinations of columns of the input. Formally, if $E_{j,v}$ is the vth element of E_j , then (\mathbf{A}, E, D) is regular if there exists a $d \times P$ matrix $\mathbf{U}_{j,v}$ and functions $\hat{E}_{j,v}$, such that $E_{j,v}(\mathbf{Y}_j) = \hat{E}_{j,v}(\mathbf{1}_d^T(\mathbf{U}_{j,v} \odot \mathbf{Y}_j))$.

When d = 1, \mathbf{Y}_j has only one row and $\mathbf{1}_d = 1$ is a scalar. Thus, $E_{j,v}(\mathbf{Y}_j) = \hat{E}_{j,v}(\mathbf{U}_{j,v} \odot \mathbf{Y}_j)$ implies that E is an arbitrary function of \mathbf{Y}_j . When d > 1, each output coordinate only depends on linear combinations of input columns. Since linear combinations do not introduce extra bits, this allows practical communication compression. We will study regular encoders E.

Redundancy Bound. We first study redundancy requirements for exact recovery of the sum of gradients with s adversaries and compression ratio r_c .

Theorem 2. A mechanism (\mathbf{A}, E, D) of gradient allocation, regular encoding, and decoding with compression ratio r_c tolerating s adversarial nodes must have a redundancy ratio $r \ge 2s + r_c$.

Thus, for any regular encoder, each gradient has to be replicated on average at least $2s+r_c$ times to defend against s adversarial nodes with a communication compression ratio of r_c . If a mechanism tolerates s adversarial nodes with a communication compression ratio of r_c , by Theorem 2, each compute node encodes at least $(2s+r_c)$ d-dimensional vectors on average. If the encoding has linear time complexity, then each encoder requires $O((2s+r_c)d)$ operations in the worst case. If the decoder D has linear time complexity,

then it requires at most $O(Pd_c)$ operations in the worst case, as it needs to use the d-dimensional input from all P compute nodes. This gives a computational cost of $O(Pd_c)$, which is less than the bound O(Pd) for the repetition code in [7].

To better understand the lower bound, we give an equivalent formulation it in the language of linear algebra. Let g be one of the $d \times 1$ dimensional gradients. Suppose it gets sent to r nodes. Then the potentially corrupted output of the linear encoder at each node j can be represented by $R_j = Z_j g + n_j$, and n_j is the noise here for $j = 1, \ldots, r$, where each Z_j is a $d_c \times d$ dimensional matrix. If the number of adversaries is at most s, then at most s vectors n_j are nonzero. We call this set of perturbation $B_{s,r}$. Thus, the goal is to design the r matrices Z_j , such that for any collection of vectors n_j at most s of which are nonzero, it is possible to recover g from the observations (Z_j, r_j) , $j = 1, \ldots, r$. Let $R := (R_1, \ldots, R_r)$ and $n := (n_1, \ldots, n_r)$, which we view as a concatenation of vectors belonging to the allowed set $B_{s,r}$. For the recovery of g to be possible, we need that if R(g,n) = R(g',n') for $g,g' \in \mathbb{R}^d$ and $g,n' \in B_{s,r}$, then g = g'.

We can write R as a linear function R=Zg+n, where Z is an $rd_c\times d$ concatenation of the matrices Z_i . Thus, we can write R(g,n)=R(g',n') as $Zg+n=Zg'+n'\iff Z(g-g')=n-n'$. Moreover, we have $n''=n-n'\in B_{2s,r}$, because at most 2s of its P sub-vectors of size d_c are nonzero. Clearly, all vectors in $B_{2s,r}$ can be written in this form. Denoting x=g-g', the problem is to understand when there exists a matrix Z such that for all $x\in\mathbb{R}^d$, we have $Zx\notin B_{2s,r}$. Now, $B_{2s,r}$ is a union of several $2sd_c$ -dimensional linear subspaces in rd_c dimensions. Moreover, Zx belongs to span(Z), which is an at most d-dimensional subspace in rd_c dimensions. Thus, for this to be possible, by counting dimensions we obtain that we need $rd_c\geq 2sd_c+d$. Since $r_c=d/d_c$, this is equivalent to $r\geq 2s+r_c$. This finishes the proof of the fundamental lower bound on the redundancy.

3.4 Optimal Coding Schemes

Can we achieve the optimal redundancy bound with linear-time encoding and decoding? More formally, can we design a tuple (\mathbf{A}, E, D) with redundancy ratio $r = 2s + r_c$ and computation complexity $\mathcal{O}((2s + r_c)d)$ at the compute nodes and $\mathcal{O}(Pd_c)$ at the PS? We give a positive answer by designing certain *linear block codes* that match the above bounds.

This is a challenging problem. In fact, we can show (see Appendix B) that this question is *exactly equivalent* to a sparse recovery problem, where we wish to recover an unknown sparse vector from linear combinations of a fixed set of vectors [9, 8, 21]. With this lens, our algorithms are related to the classical Prony's method in signal processing [26, 43]. However, a key difference is that in our case, we have a *structured set of* perturbations, where entire sub-vectors corresponding to gradients are perturbed at the same time. We leverage this to develop algorithms faster than Prony's method.

Linear Block Code. We focus on the case when $2s + r_c$ divides P; otherwise we can change P or r_c until $2s + r_c$ divides P. Divide the compute nodes into $q := P/(2s + r_c) = P/r$ "blocks" or groups. We assign each node in the same block to compute the same gradients. Each node sends some linear combination of coordinates of the assigned gradients to the PS ("linear"). The PS solves systems of linear equations to get the desired gradient sum. Following the convention of coding theory [47], we call our approach *linear block codes*.

The linear block code $(\mathbf{A}, E, D) = (\mathbf{A}^{LBC}, E^{LBC}, D^{LBC})$ is defined as follows. The assignment matrix is $\mathbf{A} = \mathbf{I}_q \otimes \mathbf{1}_{r \times r}$.

The jth compute node first selects its allocated gradients $\mathbf{Y}_j = (\mathbf{1}_d \mathbf{A}_{j,\cdot}) \odot \mathbf{G}$. Its encoder function sums up the allocated gradients into $\mathbf{Y}_j \mathbf{1}_P$, then computes and sends $\mathbf{z}_j = E_j(\mathbf{Y}_j) = \mathbf{W}_j \mathbf{Y}_j \mathbf{1}_P$ to the PS, where \mathbf{W}_j is a $d_c \times d$ matrix.

The decoder function, summarized in Algorithm 1, partitions the received updates into the q blocks computing identical gradients. For each, a block decoder $\psi(\cdot,\cdot)$ is called to recover the sum of all gradients in this group.

There are three questions left: (i) how \mathbf{W}_j is constructed, (ii) how the adversarial node index location function $\phi(\cdot)$ works, and (iii) how the block decoder function $\psi(\cdot, \cdot)$ works.

Algorithm 1 Decoder Function *D*.

```
Input: Received d_c \times P matrix \mathbf{R} Output: Desired gradient summation \mathbf{u}

1 Let \mathbf{R} = [\mathbf{R}_1, \mathbf{R}_2, \cdots, \mathbf{R}_q], where each \mathbf{R}_j is a d_c \times r matrix

2 for j=1 to q do

3 V = \phi(\mathbf{R}_j, j) // Locate the adversarial nodes
V = \{1, 2, \cdots, r\} \setminus V // Non-adversarial nodes
\mathbf{u}_j = \psi(\mathbf{R}_j, j, U) // Decode each block using the non-adversarial nodes

4 end

5 Compute and return \mathbf{u} = \sum_{i=1}^q \mathbf{u}_i
```

Given any distinct nonzero scalars w_1, w_2, \cdots, w_P , we propose to construct \mathbf{W}_j as $\mathbf{W}_j \triangleq \mathbf{I}_{d_c} \otimes [1, w_j, w_j^2, \cdots, w_j^{r_c-1}]$. The adversarial node index locating function $\phi(\cdot)$ works as follows. Given the $d_c \times r$ matrix \mathbf{R}_j received from the compute nodes, we first generate a $1 \times d_c$ random vector $\mathbf{f} \sim \mathcal{N}(\mathbf{1}_{1 \times d_c}, \mathbf{I}_d)$, and then compute $\mathbf{r}_{j,c} \triangleq \mathbf{f}\mathbf{R}_j$. Next, we obtain an r-dimensional vector $\mathbf{a} = [a_1, a_2, \cdots, a_r]$ by solving the linear system $\left[\hat{\mathbf{W}}_{j,r_c+s-1}, -\hat{\mathbf{W}}_{j,s-1} \odot (\mathbf{r}_{j,c}^T \mathbf{1}_s^T)\right] \mathbf{a} = \mathbf{r}_{j,c} \odot \left[\hat{\mathbf{W}}_{j,s}\right]_{..s}$, where

$$\hat{\mathbf{W}}_{j,v} \triangleq \begin{bmatrix} 1 & w_{(j-1)r+1} & w_{(j-1)r+1}^2 & \cdots & w_{(j-1)r+1}^v \\ 1 & w_{(j-1)r+2} & w_{(j-1)r+2}^2 & \cdots & w_{(j-1)r+2}^v \\ \vdots & \vdots & \vdots & \vdots & \vdots \\ 1 & w_{jr} & w_{jr}^2 & \cdots & w_{jr}^v \end{bmatrix}.$$

Finally compute $P_j(w) \triangleq (\sum_{i=0}^{r_c+s-1} a_{i+1} w^i)/(w^s + \sum_{i=0}^{s-1} a_{i+r_c+s+1} w^i)$, and return $V = \{i | P_j(w_{(r-1)j+i}) \neq [\mathbf{r}_{j,c}]_i\}$. The decoding function $\psi(\cdot,\cdot)$ computes and returns $vec\left([\mathbf{R}_j]_{\cdot,U} \left[\hat{W}_{j,r_c-1}\right]_{U,\cdot}^{-1,T}\right)$ given the non-adversarial node indices U.

The following lemma ensures that the Byzantine nodes are correctly found.

Lemma 3. Suppose $|\{j: \|\mathbf{n}_j\|_0 \neq 0\}| \leq s$ and $r \geq r_c + 2s$. Then $\phi(\mathbf{R}_j, j) = \{i: \|\mathbf{n}_{j(r-1)+i}\|_0 \neq 0\}$ with probability equal to unity.

The next lemma demonstrates that within each group the gradient is correctly recovered.

Lemma 4. If U consists solely of at least r-s non-adversarial nodes, then with probability equal to unity, $\mathbf{u}_j = \sum_{k=(j-1)r+1}^{jr} \mathbf{y}_k$.

Combing the above two results, we show that the linear block code tolerates any s adversaries, achieving the optimal redundancy and compression ratio with linear-time encoding and decoding.

Theorem 5. The linear block code (\mathbf{A}, E, D) tolerates any s adversaries with probability equal to unity, and achieves the redundancy ratio bound. For $d \gg P$, its encoding and decoding achieve linear-time computational complexity.

Theorem 5 shows that the linear block code is information theoretically tight and enjoys a small computational overhead even for large ML models.

4 Experiments

Now we present an empirical study on SOLON compared with several existing methods including DRACO [7], BULYAN [23], and SIGNUM [5]. Across diverse ML models trained on real world datasets, we have found 1) that SOLON results in significant speedups over existing methods, including $10\times$ faster than BULYAN and 80% faster than DRACO while reaching the same accuracy, and 2) that SOLON consistently leads to successful convergence for all Byzantine attacks considered, while previous approaches may fail on different attacks (e.g., SIGNUM on constant attack, and BULYAN on "A little is enough" (ALIE) attack [4]).

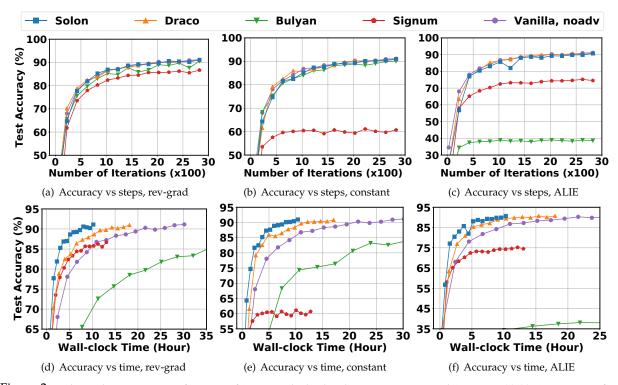


Figure 2: End to end convergence performance of SOLON and other baselines on ResNet-18 and CIFAR-10. (a)-(c): Comparison of test accuracy vs. the number of iterations between SOLON $r_c=10$ and other methods under different attacks. (d)-(f): Test accuracy vs. running time of SOLON and other methods. Vanilla SGD simply averages gradients received on PS and is tested without adversary. Accuracy may fluctuate occasionally due to randomness and lr adjustments.

Experimental setup. We implement SOLON in PyTorch [41] with MPI [11]. The experiments were conducted on a cluster of 50 real machines from Cloudlab [19] with 1 Gbps network speed and 100 virtual compute nodes. We trained three large scale models, namely, ResNet-18 [24] on CIFAR-10 [31], VGG13-BN [46] on SVHN [40], and a two-layer stacked LSTM [25] (nhid=200) on WikiText-2 [39], respectively. The details are summarized in Table 1. For comparison with SOLON, we also evaluate two robust aggregator-based approachs, BULYAN, SIGNUM, and an algorithmic redundancy-based approach, DRACO. SOLON splits the virtual machines evenly into 5 groups, each with 20 redundant machines. To compare with the best possible performance of DRACO, we set the r=11 and only use 5 groups for DRACO to reduce its communication overhead. More details are in the appendix.

Table 1: Summary of the datasets, models, and hyper-parameters used in our experiments.

Dataset	CIFAR-10	SVHN	WikiText-2
# data points	60,000	600,000	2,551,843
Model	ResNet-18	VGG13-BN	LSTM
# Parameters	11,173k	9,923k	7,332k
Optimizer	SGD	SGD	SGD
Batch Size	120	120	60

Table 2: The size of gradients to transmit per worker before and after compression (MB, 10^6 bytes).

Model	ResNet18	VGG13	LSTM
Size	89.6	79.4	58.8
$r_c = 6$	14.9	13.2	9.78
$r_c = 8$	11.2	9.92	7.35
$r_c = 10$	8.96	7.94	5.88

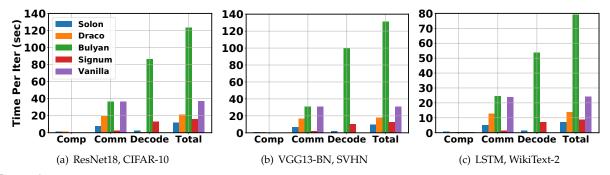


Figure 3: Time breakdown per iteration of SOLON $r_c = 10$ and all baseline methods over three models+datasets under rev-grad. The types of attack will not affect most of the times. Notice that even if SIGNUM is the fastest in time per iteration among those methods, and even faster than vanilla SGD, its accuracy is sacrificed and thus SOLON still has the best convergence performance.

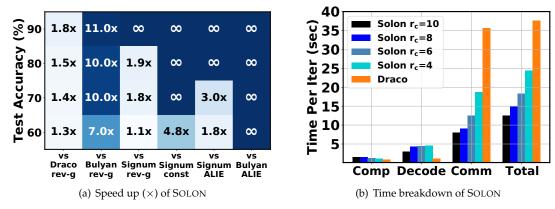


Figure 4: (a) The speed up (\times) of SOLON, $r_c=10$ vs other baselines on converging to certain test accuracy level on ResNet-18+CIFAR-10 under selected attacks. Values are approximation. ∞ means the method does not converge to the accuracy in the experiment. (b) Time breakdown of SOLON by varying r_c , fixing s with similar # of compute nodes on ResNet-18 trained over the CIFAR-10 dataset (regardless of attacks).

Attacks. We use three different attacks: reverse gradient, constant, and ALIE ("A little is enough" [4]). In the reverse gradient attack (rev-grad), Byzantine nodes always send κ times the true gradient to the PS. In the constant attack, Byzantine nodes always send a constant multiple c of the all-ones vector. In the experiments shown, $\kappa = -100$ and c = -100.

In ALIE, Byzantine nodes use local information to estimate the mean and variance of the gradients computed at the other nodes, and then manipulate the gradient as $\hat{\mu} + z \cdot \hat{\sigma}$ where $\hat{\mu}$ and $\hat{\sigma}$ are the mean and standard deviation of the gradients estimated by Byzantine nodes and z is an adjustable hyper-parameter that adds an unnoticeable perturbation to disrupt the aggregation. In experiments, we set z=1. At each iteration, we randomly select s=5 compute nodes as adversaries.

End to end performance. We start by evaluating SOLON's end to end performance along with the baseline methods under different attacks, which is shown in Figure 2. We first note that previous approaches may result in significant accuracy loss under certain attacks. For example, SIGNUM's accuracy is 30% worse than the Byzantine-free vanilla SGD under constant attack (Figure 2(b)), and ALIE attack leads a 50% accuracy drops for BULYAN (Figure 2(c)). Nevertheless, across different attacks, SOLON consistently converges and matches the accuracy performance of the vanilla SGD in a Byzantine-free environment. This is primarily due to SOLON's black box performance guarantee.

Furthermore, SOLON provides significant runtime speedups over existing methods. For example, as shown in Figure 2(d), SOLON converges faster than all the other Byzantine-resilient approaches. Its runtime performance even outperforms the vanilla SGD in a Byzantine-free environment. This is primarily due to

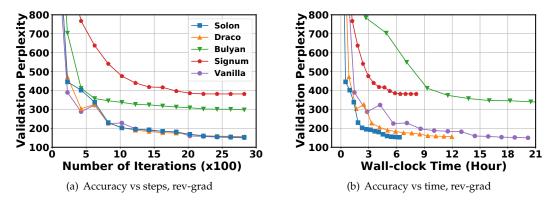


Figure 5: End to end convergence performance of SOLON $r_c = 10$ and other baselines on LSTM model trained over WikiText-2 dataset under reverse gradient attack, s = 5. (a) Validation perplexity vs. # iterations. (b) Validation perplexity vs. running time.

the communication efficiency of SOLON. We observe a similar trend for the other two models (e.g., LSTM under rev-grad attack shown in Figure 5). Figure 4(a) gives a quantitative result of the speedups achieved by SOLON. To achieve a 90% test accuracy, SOLON obtains a speedup of $1.8\times$ over DRACO and $11\times$ over BULYAN under the reverse gradient attack, while SIGNUM cannot reach 90% accuracy. Other details and results can be found in the Appendix.

Per iteration cost. Next, we dive into the per iteration cost of each approach. As shown in Figure 3. We note that BULYAN requires a significantly higher decoding time than all the other methods. This is probably because BULYAN deploys a computational expensive robust aggregator. Note that SOLON reduces the communication cost by slightly increasing the computation and decoding complexity compared to DRACO. Nevertheless, across all datasets and models considered in our experiments, SOLON attains the fastest per iteration runtime. This is because SOLON largely reduces the communication cost, which is the bottleneck in a large cluster, and the extra computation and decoding cost is relatively small.

Effects of compression ratio. Finally we evaluate the effects of the compression ratio r_c on SOLON's performance, as shown in Figure 4(b). Here we vary compression rate r_c , fix attacks s, and change redundancy ratio r accordingly. We keep the entire number of machines roughly at the same level by varying group numbers. Overall, as the compression ratio decreases, the communication cost increases almost linearly, and thus the total runtime. This shows that SOLON can be applied for different communication requirements with small extra overhead. In addition, we observe that the computation cost increases slightly when r_c goes up, since the increase of r_c will require an increase in the group batch size. The decode time also changes slightly. However, these are not major factors compared to communication. Other details can be found in the appendix.

In addition, we also evaluate the size of the gradients before and after compression, summarized in Table 2. Overall, SOLON largely reduces the gradient size up to $10\times$, depending on the specified compression ratio r_c . In fact, SOLON allows users to specify the compression ratio explicitly to satisfy different clusters' requirements.

5 Conclusion

In this paper, we propose SOLON, a distributed training framework that simultaneously resists Byzantine attack and reduces communication overhead via algorithmic redundancy. We show that there is a fundamental trade-off between Byzantine-resilience, communication cost, and computational cost. Extensive experiments show that SOLON provides significant speedups over existing methods, and consistently leads to successful convergence under different attacks.

References

- [1] Saurabh Agarwal, Hongyi Wang, Kangwook Lee, Shivaram Venkataraman, and Dimitris Papailiopoulos. Accordion: Adaptive gradient communication via critical learning regime identification. *arXiv* preprint *arXiv*:2010.16248, 2020.
- [2] Dan Alistarh, Demjan Grubic, Jerry Li, Ryota Tomioka, and Milan Vojnovic. Qsgd: Communication-efficient sgd via gradient quantization and encoding. *arXiv preprint arXiv:1610.02132*, 2016.
- [3] Dan Alistarh, Demjan Grubic, Jerry Li, Ryota Tomioka, and Milan Vojnovic. Qsgd: Communication-efficient sgd via gradient quantization and encoding. In *Advances in Neural Information Processing Systems*, pages 1707–1718, 2017.
- [4] Gilad Baruch, Moran Baruch, and Yoav Goldberg. A little is enough: Circumventing defenses for distributed learning. In H. Wallach, H. Larochelle, A. Beygelzimer, F. d Alché-Buc, E. Fox, and R. Garnett, editors, *Advances in Neural Information Processing Systems*, volume 32, pages 8635–8645, 2019.
- [5] Jeremy Bernstein, Jiawei Zhao, Kamyar Azizzadenesheli, and Anima Anandkumar. signSGD with majority vote is communication efficient and fault tolerant. In *ICLR*, 2019.
- [6] Peva Blanchard, Rachid Guerraoui, Julien Stainer, et al. Machine learning with adversaries: Byzantine tolerant gradient descent. In *Advances in Neural Information Processing Systems*, pages 119–129, 2017.
- [7] Lingjiao Chen, Hongyi Wang, Zachary Charles, and Dimitris Papailiopoulos. Draco: Byzantine-resilient distributed training via redundant gradients. In *International Conference on Machine Learning*, pages 903–912, 2018.
- [8] Scott Shaobing Chen, David L Donoho, and Michael A Saunders. Atomic decomposition by basis pursuit. *SIAM review*, 43(1):129–159, 2001.
- [9] Shaobing Chen and David Donoho. Basis pursuit. In *Proceedings of 1994 28th Asilomar Conference on Signals, Systems and Computers*, volume 1, pages 41–44. IEEE, 1994.
- [10] Yudong Chen, Lili Su, and Jiaming Xu. Distributed statistical machine learning in adversarial settings: Byzantine gradient descent. *Proceedings of the ACM on Measurement and Analysis of Computing Systems*, 1(2):1–25, 2017.
- [11] Lisandro Dalcín, Rodrigo Paz, and Mario Storti. Mpi for python. *Journal of Parallel and Distributed Computing*, 65(9):1108–1115, 2005.
- [12] Georgios Damaskinos, El-Mahdi El-Mhamdi, Rachid Guerraoui, Arsany Guirguis, and Sébastien Rouault. AGGREGATHOR: byzantine machine learning via robust gradient aggregation. In Ameet Talwalkar, Virginia Smith, and Matei Zaharia, editors, *MLSys*, 2019.
- [13] Jeffrey Dean, Greg Corrado, Rajat Monga, Kai Chen, Matthieu Devin, Mark Mao, Andrew Senior, Paul Tucker, Ke Yang, Quoc V Le, et al. Large scale distributed deep networks. In *Advances in Neural Information Processing Systems*, pages 1223–1231, 2012.
- [14] Jeffrey Dean, Greg Corrado, Rajat Monga, Kai Chen, Matthieu Devin, Mark Mao, Andrew Senior, Paul Tucker, Ke Yang, Quoc V Le, et al. Large scale distributed deep networks. In *Advances in Neural Information Processing Systems*, pages 1223–1231, 2012.
- [15] Jia Deng, Wei Dong, Richard Socher, Li-Jia Li, Kai Li, and Li Fei-Fei. Imagenet: A large-scale hierarchical image database. In *CVPR*, pages 248–255. Ieee, 2009.
- [16] Jacob Devlin, Ming-Wei Chang, Kenton Lee, and Kristina Toutanova. BERT: pre-training of deep bidirectional transformers for language understanding. In Jill Burstein, Christy Doran, and Thamar Solorio, editors, *NAACL*, 2019.

- [17] Edgar Dobriban and Yue Sheng. Wonder: Weighted one-shot distributed ridge regression in high dimensions. *Journal of Machine Learning Research*, 21(66):1–52, 2020.
- [18] Edgar Dobriban and Yue Sheng. Distributed linear regression by averaging. *The Annals of Statistics*, 49(2):918–943, 2021.
- [19] Dmitry Duplyakin, Robert Ricci, Aleksander Maricq, Gary Wong, Jonathon Duerig, Eric Eide, Leigh Stoller, Mike Hibler, David Johnson, Kirk Webb, Aditya Akella, Kuangching Wang, Glenn Ricart, Larry Landweber, Chip Elliott, Michael Zink, Emmanuel Cecchet, Snigdhaswin Kar, and Prabodh Mishra. The design and operation of CloudLab. In *Proceedings of the USENIX Annual Technical Conference (ATC)*, pages 1–14, July 2019.
- [20] El-Mahdi El-Mhamdi, Rachid Guerraoui, Arsany Guirguis, Lê Nguyên Hoang, and Sébastien Rouault. Genuinely distributed byzantine machine learning. In *Proceedings of the 39th Symposium on Principles of Distributed Computing*, PODC '20, page 355–364, New York, NY, USA, 2020. Association for Computing Machinery.
- [21] Michael Elad. *Sparse and redundant representations: from theory to applications in signal and image processing.* Springer Science & Business Media, 2010.
- [22] Avishek Ghosh, Raj Kumar Maity, Swanand Kadhe, Arya Mazumdar, and Kannan Ramchandran. Communication-efficient and byzantine-robust distributed learning. In 2020 Information Theory and Applications Workshop (ITA), pages 1–28. IEEE, 2020.
- [23] Rachid Guerraoui, Sébastien Rouault, et al. The hidden vulnerability of distributed learning in byzantium. In *International Conference on Machine Learning*, pages 3521–3530, 2018.
- [24] Kaiming He, Xiangyu Zhang, Shaoqing Ren, and Jian Sun. Deep residual learning for image recognition. In *CVPR*, pages 770–778, 2016.
- [25] Sepp Hochreiter and Jürgen Schmidhuber. Lstm can solve hard long time lag problems. In *Proceedings of the 9th International Conference on Neural Information Processing Systems*, Advances in Neural Information Processing Systems, page 473–479. MIT Press, 1996.
- [26] M Hurst and Raj Mittra. Scattering center analysis via prony's method. *IEEE Transactions on Antennas and Propagation*, 35(8):986–988, 1987.
- [27] Yimin Jiang, Yibo Zhu, Chang Lan, Bairen Yi, Yong Cui, and Chuanxiong Guo. A unified architecture for accelerating distributed DNN training in heterogeneous gpu/cpu clusters. In *OSDI*, pages 463–479, 2020.
- [28] Rie Johnson and Tong Zhang. Accelerating stochastic gradient descent using predictive variance reduction. In *Advances in Neural Information Processing Systems*, pages 315–323, 2013.
- [29] Sai Praneeth Karimireddy, Lie He, and Martin Jaggi. Learning from history for byzantine robust optimization. *CoRR*, abs/2012.10333, 2020.
- [30] Jakub Konečný, H Brendan McMahan, Felix X Yu, Peter Richtárik, Ananda Theertha Suresh, and Dave Bacon. Federated learning: Strategies for improving communication efficiency. *arXiv* preprint *arXiv*:1610.05492, 2016.
- [31] Alex Krizhevsky and Geoffrey Hinton. Learning multiple layers of features from tiny images. 2009.
- [32] Leslie Lamport, Robert Shostak, and Marshall Pease. The byzantine generals problem. In *Concurrency: the Works of Leslie Lamport*, pages 203–226. 2019.
- [33] P.D. Lax. *Linear Algebra and Its Applications*. Pure and Applied Mathematics: A Wiley Series of Texts, Monographs and Tracts. Wiley, 2007.

- [34] Mu Li, David G Andersen, Jun Woo Park, Alexander J Smola, Amr Ahmed, Vanja Josifovski, James Long, Eugene J Shekita, and Bor-Yiing Su. Scaling distributed machine learning with the parameter server. In *OSDI*, pages 583–598, 2014.
- [35] Mu Li, David G Andersen, Alexander J Smola, and Kai Yu. Communication efficient distributed machine learning with the parameter server. In *Advances in Neural Information Processing Systems*, volume 2, pages 1–4, 2014.
- [36] Mu Li, Li Zhou, Zichao Yang, Aaron Li, Fei Xia, David G Andersen, and Alexander Smola. Parameter server for distributed machine learning. In *Big Learning NIPS Workshop*, volume 6, page 2, 2013.
- [37] Yujun Lin, Song Han, Huizi Mao, Yu Wang, and William J Dally. Deep gradient compression: Reducing the communication bandwidth for distributed training. *arXiv preprint arXiv:1712.01887*, 2017.
- [38] Brendan McMahan, Eider Moore, Daniel Ramage, Seth Hampson, and Blaise Aguera y Arcas. Communication-efficient learning of deep networks from decentralized data. In *AISTATS*, pages 1273–1282. PMLR, 2017.
- [39] Stephen Merity, Caiming Xiong, James Bradbury, and Richard Socher. Pointer sentinel mixture models. *arXiv preprint arXiv:1609.07843*, 2016.
- [40] Yuval Netzer, Tao Wang, Adam Coates, Alessandro Bissacco, Bo Wu, and Andrew Ng. Reading digits in natural images with unsupervised feature learning. *NIPS Workshop on Deep Learning and Unsupervised Feature Learning*, 01 2011.
- [41] Adam Paszke, Sam Gross, Francisco Massa, Adam Lerer, James Bradbury, Gregory Chanan, Trevor Killeen, Zeming Lin, Natalia Gimelshein, Luca Antiga, et al. Pytorch: An imperative style, high-performance deep learning library. In *Advances in Neural Information Processing Systems*, 2019.
- [42] Shashank Rajput, Hongyi Wang, Zachary Charles, and Dimitris Papailiopoulos. DETOX: A redundancy-based framework for faster and more robust gradient aggregation. In H. Wallach, H. Larochelle, A. Beygelzimer, F. d Alché-Buc, E. Fox, and R. Garnett, editors, *NeurIPS*, volume 32, pages 10320–10330. Curran Associates, Inc., 2019.
- [43] Benjamin Recht. Prony's method. CS838 Topics in optimization: Convex geometry in high-dimensional data analysis, Lecture 6, 2010.
- [44] Frank Seide, Hao Fu, Jasha Droppo, Gang Li, and Dong Yu. 1-bit stochastic gradient descent and its application to data-parallel distributed training of speech dnns. In *Fifteenth Annual Conference of the International Speech Communication Association*, 2014.
- [45] Alexander Sergeev and Mike Del Balso. Horovod: fast and easy distributed deep learning in tensorflow. *arXiv preprint arXiv:1802.05799*, 2018.
- [46] Karen Simonyan and Andrew Zisserman. Very deep convolutional networks for large-scale image recognition. In Yoshua Bengio and Yann LeCun, editors, ICLR 2015, San Diego, CA, USA, May 7-9, 2015, Conference Track Proceedings, 2015.
- [47] Bernard Sklar and F.J. Harris. The abcs of linear block codes. *Signal Processing Magazine*, *IEEE*, 21:14 35, 08 2004.
- [48] Sebastian U Stich, Jean-Baptiste Cordonnier, and Martin Jaggi. Sparsified sgd with memory. *arXiv* preprint arXiv:1809.07599, 2018.
- [49] Ananda Theertha Suresh, X Yu Felix, Sanjiv Kumar, and H Brendan McMahan. Distributed mean estimation with limited communication. In *Internation Conference on Machine Learning*, pages 3329–3337. PMLR, 2017.

- [50] Rashish Tandon, Qi Lei, Alexandros G Dimakis, and Nikos Karampatziakis. Gradient coding: Avoiding stragglers in distributed learning. In *International Conference on Machine Learning*, pages 3368–3376, 2017.
- [51] V. Vapnik. Principles of risk minimization for learning theory. In J. Moody, S. Hanson, and R. P. Lippmann, editors, *Advances in Neural Information Processing Systems*, volume 4. Morgan-Kaufmann, 1992.
- [52] Vladimir Vapnik. The nature of statistical learning theory. Springer science & business media, 2013.
- [53] Thijs Vogels, Sai Praneeth Karimireddy, and Martin Jaggi. Powersgd: Practical low-rank gradient compression for distributed optimization. *Advances in Neural Information Processing Systems*, 32:14259–14268, 2019.
- [54] Hongyi Wang, Scott Sievert, Shengchao Liu, Zachary B. Charles, Dimitris S. Papailiopoulos, and Stephen Wright. ATOMO: communication-efficient learning via atomic sparsification. In Samy Bengio, Hanna M. Wallach, Hugo Larochelle, Kristen Grauman, Nicolò Cesa-Bianchi, and Roman Garnett, editors, *Advances in Neural Information Processing*, pages 9872–9883, 2018.
- [55] Wei Wen, Cong Xu, Feng Yan, Chunpeng Wu, Yandan Wang, Yiran Chen, and Hai Li. Terngrad: Ternary gradients to reduce communication in distributed deep learning. *arXiv preprint arXiv:1705.07878*, 2017.
- [56] Cong Xie, Oluwasanmi Koyejo, and Indranil Gupta. Fall of empires: Breaking byzantine-tolerant sgd by inner product manipulation. In *Uncertainty in Artificial Intelligence*, pages 261–270. PMLR, 2020.
- [57] Cong Xie, Sanmi Koyejo, and Indranil Gupta. Zeno: Distributed stochastic gradient descent with suspicion-based fault-tolerance. In Kamalika Chaudhuri and Ruslan Salakhutdinov, editors, *Proceedings of the 36th International Conference on Machine Learning*, volume 97 of *Proceedings of Machine Learning Research*, pages 6893–6901. PMLR, 2019.
- [58] Min Ye and Emmanuel Abbe. Communication-computation efficient gradient coding. In *Internation Conference on Machine Learning*, volume 80, pages 5610–5619. PMLR, 10–15 Jul 2018.
- [59] Dong Yin, Yudong Chen, Ramchandran Kannan, and Peter Bartlett. Byzantine-robust distributed learning: Towards optimal statistical rates. In *Internation Conference on Machine Learning*, pages 5650–5659. PMLR, 2018.

Outline The supplement materials are organized as follows. All proofs are first presented in Section A. In addition, we provide a short discussion on how the Byzantine recovery problem is related to sparse recovery in Section B. Section C and D give the details of experimental setups and additional empirical findings, respectively. Finally, we discuss the limitation and potential societal impact in more detail in Section E.

A Proofs

A.1 Proof of Theorem 1

Proof. For $k=1,2,\ldots,d/r_c$, $j=\ldots,1,0,-1,\ldots$, and $\ell=1,2,\ldots,r_c$, define two functions $f_{1,r_c}(\cdot):\mathbb{R}^d\to\mathbb{R}^{d/r_c}$ and $f_{-1,r_c}(\cdot):\mathbb{R}^{d/r_c}\to\mathbb{R}^d$ as

$$\lceil f_{1,r_c}(x_1, x_2, \dots, x_d)_k / 10^{r_c j + \ell} \rceil \mod 10 \equiv \lceil x_{(k-1)r_c + \ell} / 10^j \rceil \mod 10$$

$$\lceil f_{-1,r_c}(y_1, y_2, \dots, y_{d/r_c})_{r_c(k-1)+\ell}/10^j \rceil \mod 10 \equiv \lceil y_k/10^{r_cj+\ell} \rceil \mod 10.$$

The second subscript of the functions, k, and $r_c(k-1) + \ell$, respectively, denotes the kth and $r_c(k-1) + \ell$ th output of the functions.

The function $f_{1,r_c}(\cdot)$ compresses a d-dimensional vector by cascading all digits of each element of the input into a long vector, and $f_{-1,r_c}(\cdot)$ reverses the process. For example, if $x_1=123, x_2=456, x_3=789$, and $d=r_c=3$, then $f_{1,r_c}(x_1,x_2,x_3)=9638529630$. Given $y_1=9638529630$ and $d=r_c=3$, we have $f_{-1,r_c}(y_1)=(123,456,789)$. In general, we have the following lemma.

Lemma 6 (The two functions are inverses.). $f_{-1,r_c}(f_{1,r_c}(x_1,x_2,...,x_d)) = (x_1,x_2,...,x_d)$.

Proof. Let $z_k = f_{1,r_c}(x_1, x_2, ..., x_d)_k$. We have

$$\lceil f_{-1,r_c}(z_1, z_2, \dots, z_{d/r_c})_{r_c(k-1)+\ell} / 10^j \rceil \mod 10 \equiv \lceil z_k / 10^{r_c j + \ell} \rceil \mod 10$$

and by definition of z_k , we have

$$\lceil z_k/10^{r_cj+\ell} \rceil \mod 10 \equiv \lceil x_{(k-1)r_c+\ell}/10^j \rceil \mod 10.$$

Thus, we have for all j

$$\lceil f_{-1,r_c}(z_1, z_2, \dots, z_{d/r_c})_{r_c(k-1)+\ell} / 10^j \rceil \mod 10 \equiv \lceil z_k / 10^{r_c j + \ell} \rceil \mod 10
\equiv \lceil x_{(k-1)r_c + \ell} / 10^j \rceil \mod 10.$$

Therefore, each digit of $f_{-1,r_c}(z_1,z_2,\ldots,z_{d/r_c})_{r_c(k-1)+\ell}$ is the same as that of $x_{r_c(k-1)+\ell}$. Hence, we must have $f_{-1,r_c}(z_1,z_2,\ldots,z_{d/r_c})_{r_c(k-1)+\ell} = x_{r_c(k-1)+\ell}$, which holds for $k=1,2,\ldots,d/r_c,\ell=1,2,\ldots,r_c$. Thus, we have $f_{-1,r_c}(f_{1,r_c}(x_1,x_2,\ldots,x_d)) = (x_1,x_2,\ldots,x_d)$, which finishes the proof.

Now we are ready to construct (A', E', D'). Given (A, E, D), we let $A' \triangleq A$, $E'_j(\mathbf{Y}_j) \triangleq f_{1,r_c}(E_j(\mathbf{Y}_j))$, and $D'_j(\mathbf{R}) \triangleq D(f_{-1,r_c}(\mathbf{R}_1), f_{-1,r_c}(\mathbf{R}_2), \dots, f_{-1,r_c}(\mathbf{R}_P))$. By definition, it is clear that the constructed (A', E', D') compresses the size of vectors (or also the communication cost) by a factor of r_c . The remaining part is to prove that (A', E', D') can resist s adversarial nodes. W.l.o.g., assume the first P-2s nodes are not Byzantine. Then we have $\mathbf{R}_j = f_{1,r_c}(E(\mathbf{Y}_j))$, and thus $f_{-1,r_c}(\mathbf{R}_j) = f_{-1,r_c}(f_{1,r_c}(E(\mathbf{Y}_j))) = E_j(\mathbf{Y}_j), j = 1, 2, \dots, P-2s$. Hence, we have $D'(\mathbf{R}) = D(E_1(\mathbf{Y}_1), E_2(\mathbf{Y}_2), \dots, E_{P-2s}(\mathbf{Y}_{P-2s}), \mathbf{R}_{P-2s+1}, \dots, \mathbf{R}_P)$. Since (A, E, D) can resist s Byzantine nodes, given P-2s correctly received parts $E_j(\mathbf{Y}_j), j = 1, 2, \dots, P-2s$ and 2s arbitrary parts, the decoder should return the correct gradient sum. In other words, we have $D(E_1(\mathbf{Y}_1), E_2(\mathbf{Y}_2), \dots, E_{P-2s}(\mathbf{Y}_{P-2s}), \mathbf{R}_{P-2s+1}, \dots, \mathbf{R}_P) = \sum_{i=1}^P \mathbf{g}_i$ for any $\mathbf{R}_{P-2s+1}, \mathbf{R}_{P-2s+2}, \dots, \mathbf{R}_P$. Thus, $D'(\mathbf{R}) = \sum_{i=1}^P \mathbf{g}_i$, which demonstrates that (A', E', D') can resist s Byzantine nodes.

A.2 Proof of Theorem 2

Proof. We define a valid s-attack first.

Definition 3. The matrix $\mathbf{N} = [\mathbf{n}_1, \mathbf{n}_2, \dots, \mathbf{n}_P]$ is a valid s-attack if and only if $|\{j : ||\mathbf{n}_j||_0 \neq 0\}| \leq s$.

Suppose (\mathbf{A}, E, D) can resist s adversaries. The goal is to prove $\|\mathbf{A}\|_0 \ge P(2s+r_c)$. In fact we can prove a slightly stronger claim: $\|\mathbf{A}_{\cdot,i}\|_0 \ge (2s+r_c)$, $i=1,2,\ldots,B$. Suppose for some i, $\|\mathbf{A}_{\cdot,i}\|_0 = \tau < (2s+r_c)$. Without loss of generality, assume that $\mathbf{A}_{1,i}, \mathbf{A}_{2,i}, \ldots, \mathbf{A}_{\tau,i}$ are nonzero. Let $\mathbf{G}_{-i} = [\mathbf{g}_1, \mathbf{g}_2, \ldots, \mathbf{g}_{i-1}, \mathbf{g}_{i+1}, \ldots, \mathbf{g}_P]$. Since (\mathbf{A}, E, D) can protect against s adversaries, we have for any \mathbf{G} ,

$$D(\mathbf{Z}^{\mathbf{A},E,\mathbf{G}} + \mathbf{N}) = \mathbf{G}\mathbf{1}_P = \mathbf{G}_{-i}\mathbf{1}_{P-1} + \mathbf{g}_i,$$

for any valid s-attack N. Our goal is to show a contradiction based on the above equation.

Recall that for regular encoders, $E_{j,v}(\mathbf{Y}_j) = \hat{E}_{j,v}(\mathbf{1}_d^T(\mathbf{U}_{j,v} \odot \mathbf{Y}_j))$. Let $\mathbf{u}_{j,v}$ be the ith column of $\mathbf{U}_{j,v}$ and $\hat{\mathbf{U}} \triangleq [\mathbf{u}_{1,1}, \mathbf{u}_{1,2}, \dots, \mathbf{u}_{1,d_c}, \mathbf{u}_{2,1}, \dots, \mathbf{u}_{2,d_c}, \dots, \mathbf{u}_{\tau-2s,d_c}]$. Note that

$$\tau < 2s + r_c \Leftrightarrow \tau - 2s < r_c \Leftrightarrow (\tau - 2s)d_c < r_c d_c = d.$$

Since $\hat{\mathbf{U}}$ is a $d \times (\tau - 2s)d_c$ matrix, $\hat{\mathbf{U}}$ is not of full row rank. Therefore, there exists a d-dimensional vector $\hat{\mathbf{x}} \neq \mathbf{0}$ such that $\hat{\mathbf{U}}^T \hat{\mathbf{x}} = 0$.

Let
$$\mathbf{g}_{i}^{1} = \mathbf{1}_{d}$$
, $\mathbf{g}_{i}^{2} = \mathbf{1}_{d} + \hat{\mathbf{x}}$, and for $a = 1, 2$

$$G^a = [g_1, g_2, \dots, g_{i-1}, g_i^a, g_{i+1}, \dots, g_P].$$

Then for any valid s-attacks N^1 , N^2

$$D(\mathbf{Z}^{\mathbf{A},E,\mathbf{G}^1} + \mathbf{N}^1) = \mathbf{G}_{-i}\mathbf{1}_{P-1} + \mathbf{1}_d.$$

and

$$D(\mathbf{Z}^{\mathbf{A},E,\mathbf{G}^2} + \mathbf{N}^2) = \mathbf{G}_{-i}\mathbf{1}_{P-1} + \mathbf{1}_d + \hat{\mathbf{x}}.$$

Now we find $\mathbf{N}^1, \mathbf{N}^2$ such that $D(\mathbf{Z}^{\mathbf{A}, E, \mathbf{G}^1} + \mathbf{N}^1) = D(\mathbf{Z}^{\mathbf{A}, E, \mathbf{G}^2} + \mathbf{N}^2)$ which then leads to a contradiction. Construct \mathbf{N}^1 and \mathbf{N}^2 by

$$\mathbf{N}_{\ell,j}^1 = \begin{cases} \left[\mathbf{Z}^{\mathbf{A},E,\mathbf{G}^2}\right]_{\ell,j} - \left[\mathbf{Z}^{\mathbf{A},E,\mathbf{G}^1}\right]_{\ell,j}, & j = \tau - 2s + 1, \tau - 2s + 2, \dots, \tau - s \\ 0, & \text{otherwise} \end{cases}$$

and

$$\mathbf{N}_{\ell,j}^2 = \begin{cases} \left[\mathbf{Z}^{\mathbf{A},E,\mathbf{G}^1}\right]_{\ell,j} - \left[\mathbf{Z}^{\mathbf{A},E,\mathbf{G}^2}\right]_{\ell,j}, & j = \tau - s + 1, \tau - s + 2, \dots, \tau \\ 0, & \text{otherwise.} \end{cases}$$

One can readily verify that N^1 , N^2 are both valid s-attacks. In addition,

$$\left[\mathbf{Z}^{\mathbf{A},E,\mathbf{G}^{1}} \right]_{\ell,j} + \mathbf{N}_{\ell,j}^{1} = \left[\mathbf{Z}^{\mathbf{A},E,\mathbf{G}^{2}} \right]_{\ell,j} + \mathbf{N}_{\ell,j}^{2}, \ j = \tau - 2s + 1, \tau - 2s + 2, \dots, \tau.$$

Since $\mathbf{A}_{j,i}=0$ for all $j>\tau$, the encoder functions of compute nodes with index $j>\tau$ do not depend on the ith gradient. Since \mathbf{G}^1 and \mathbf{G}^2 only differ in the ith gradient, the encoder function of any compute node with index $j>\tau$ has the same output. Thus, we have

$$\left[\mathbf{Z}^{\mathbf{A},E,\mathbf{G}^1}\right]_{\ell,j} + \mathbf{N}^1_{\ell,j} = \left[\mathbf{Z}^{\mathbf{A},E,\mathbf{G}^1}\right]_{\ell,j} = \left[\mathbf{Z}^{\mathbf{A},E,\mathbf{G}^2}\right]_{\ell,j} = \left[\mathbf{Z}^{\mathbf{A},E,\mathbf{G}^2}\right]_{\ell,j} + \mathbf{N}^2_{\ell,j}, \qquad j > \tau$$

¹Since *i* is fixed, we omit it from $\mathbf{u}_{j,v}$, $\hat{\mathbf{U}}$, and other quantities depending implicitly on it.

Now consider $1 \le j \le \tau - 2s$. By construction of $\hat{\mathbf{x}}$, we have $\hat{\mathbf{U}}^T\hat{\mathbf{x}} = \mathbf{0}$. That is, for $1 \le j \le \tau - 2s$, $1 \le u \le d_c$, $\mathbf{u}_{i,v}^T\hat{\mathbf{x}} = 0$, which implies

$$\mathbf{u}_{j,v}^T\mathbf{g}_i^1 = \mathbf{u}_{j,v}^T\mathbf{g}_i^1 + \mathbf{u}_{j,v}^T\hat{\mathbf{x}} = \mathbf{u}_{j,v}^T\mathbf{g}_i^2.$$

Let \mathbf{Y}_j^1 and \mathbf{Y}_j^2 be the gradients computed at the jth node for \mathbf{G}^1 and \mathbf{G}^2 , respectively. In other words, $\mathbf{Y}_j^1 = (\mathbf{1}_d \mathbf{A}_{j,\cdot}) \odot \mathbf{G}^1$ and $\mathbf{Y}_j^2 = (\mathbf{1}_d \mathbf{A}_{j,\cdot}) \odot \mathbf{G}^2$. Since \mathbf{G}^1 and \mathbf{G}^2 only differ in the ith column, \mathbf{Y}_j^1 and \mathbf{Y}_j^2 can also only differ in the ith column. Therefore, for $1 \leq j \leq \tau - 2s, 1 \leq v \leq d_c$, the vectors $\mathbf{u}_{j,v}^T \mathbf{Y}_j^1$ and $\mathbf{u}_{j,v}^T \mathbf{Y}_j^2$ can only differ in the ith column (in this case, the ith entry). But the ith column of $\mathbf{u}_{j,v}^T \mathbf{Y}_j^1$ is $\mathbf{u}_{j,v}^T \mathbf{g}_i^1$, the ith column of $\mathbf{u}_{j,v}^T \mathbf{Y}_j^2$ is $\mathbf{u}_{j,v}^T \mathbf{g}_i^2$, and we have just shown that $\mathbf{u}_{j,v}^T \mathbf{g}_i^1 = \mathbf{u}_{j,v}^T \mathbf{g}_i^2$. Thus, we must have $\mathbf{u}_{j,v}^T \mathbf{Y}_j^1 = \mathbf{u}_{j,v}^T \mathbf{Y}_j^2$ for $1 \leq j \leq \tau, 1 \leq v \leq d_c$. This implies

$$\mathbf{1}_{P}^{T}(\mathbf{U}_{j,v}\odot\mathbf{Y}_{i}^{1})=\mathbf{1}_{P}^{T}(\mathbf{U}_{j,v}\odot\mathbf{Y}_{i}^{2}),$$

which in turn implies

$$E_{j,v}(\mathbf{Y}_{j}^{1}) = \hat{E}_{j,v}(\mathbf{1}_{P}^{T}(\mathbf{U}_{j,v} \odot \mathbf{Y}_{j}^{1})) = \hat{E}_{j,v}(\mathbf{1}_{P}^{T}(\mathbf{U}_{j,v} \odot \mathbf{Y}_{j}^{1})) = E_{j,v}(\mathbf{Y}_{j}^{2}).$$

That is, $\left[\mathbf{Z}^{\mathbf{A},E,\mathbf{G}^1}\right]_{v,j} = \left[\mathbf{Z}^{\mathbf{A},E,\mathbf{G}^2}\right]_{v,j}$. Further noticing that $\mathbf{N}^1_{v,j} = \mathbf{N}^2_{v,j} = 0$ when $1 \leq j \leq \tau - 2s$, we have

$$\left[\mathbf{Z}^{\mathbf{A},E,\mathbf{G}^1}\right]_{\ell,j} + \mathbf{N}^1_{\ell,j} = \left[\mathbf{Z}^{\mathbf{A},E,\mathbf{G}^2}\right]_{\ell,j} + \mathbf{N}^2_{\ell,j}, 1 \le j \le \tau - 2s.$$

Hence, we have

$$\left[\mathbf{Z}^{\mathbf{A},E,\mathbf{G}^1}\right]_{\ell,j} + \mathbf{N}_{\ell,j}^1 = \left[\mathbf{Z}^{\mathbf{A},E,\mathbf{G}^2}\right]_{\ell,j} + \mathbf{N}_{\ell,j}^2, \qquad \forall j,$$

which shows

$$\mathbf{Z}^{\mathbf{A},E,\mathbf{G}^1} + \mathbf{N}^1 = \mathbf{Z}^{\mathbf{A},E,\mathbf{G}^2} + \mathbf{N}^2.$$

Therefore, we have

$$D(\mathbf{Z}^{\mathbf{A},E,\mathbf{G}^1} + \mathbf{N}^1) = D(\mathbf{Z}^{\mathbf{A},E,\mathbf{G}^2} + \mathbf{N}^2)$$

and thus

$$\mathbf{G}_{-1}\mathbf{1}_{P-1} + \mathbf{1}_d = D(\mathbf{Z}^{\mathbf{A},E,\mathbf{G}^1} + \mathbf{N}^1) = D(\mathbf{Z}^{\mathbf{A},E,\mathbf{G}^2} + \mathbf{N}^2) = \mathbf{G}_{-1}\mathbf{1}_{P-1} + \mathbf{1}_d + \hat{\mathbf{x}}_d$$

This gives us a contradiction. Hence, the assumption is not correct and we must have $\|\mathbf{A}_{\cdot,i}\|_0 \ge (2s+r_c)$, for $i=1,2,\ldots,P$. Thus, we must have $\|A\|_0 \ge (2s+r_c)P$.

A direct but important corollary of this theorem is a bound on the number of adversaries SOLON can resist.

Corollary 7. (\mathbf{A}, E, D) can resist at most $\frac{P-r_c}{2}$ adversarial nodes.

Proof. According to Theorem 2, the redundancy ratio is at least $2s+r_c$, meaning that every data point must be replicated at least $2s+r_c$ times. Since there are P compute nodes in total, we must have $2s+r_c \le P$, which implies $s \le \frac{P-r_c}{2}$. Thus, (\mathbf{A}, E, D) can resist at most $\frac{P-r_c}{2}$ adversaries.

This corollary implies that the communication compression ratio cannot exceed the total number of compute nodes. \Box

A.3 Proof of Lemma 3

Proof. We will omit the superscript LBC indicating the linear block code in this and the following proofs. We need a few lemmas first.

Lemma 8. Define the P-dimensional vector $\gamma \triangleq [\gamma_1, \gamma_2, \dots, \gamma_P]^T = (\mathbf{f}\mathbf{N})^T$. Then we have

$$Pr({j: \gamma_j \neq 0}) = {j: ||{\mathbf{N}_{\cdot,j}}||_0 \neq 0}) = 1.$$

Proof. Let us prove that

$$Pr(\mathbf{N}_{:,i} \neq 0 | \gamma_i \neq 0) = 1.$$

and

$$Pr(\gamma_i \neq 0 | \mathbf{N}_{\cdot,i} \neq 0) = 1.$$

for any j. Combining those two equations we prove the lemma.

The first equation is readily verified, because $\mathbf{N}_{\cdot,j}=0$ implies $\gamma_j=\mathbf{f}\mathbf{N}_{\cdot,j}=0$. For the second one, note that \mathbf{f} has entries drawn independently from the standard normal distribution. Therefore we have that $\gamma_j=\mathbf{f}\mathbf{N}_{\cdot,j}\sim\mathcal{N}(\mathbf{1}^T\mathbf{N}_{\cdot,j},\|\mathbf{N}_{\cdot,j}\|_2^2)$. Since γ_j is a random variable with a non-degenerate normal distribution when $\|\mathbf{N}_{\cdot,j}\|_2^2\neq 0$, which has an absolutely continuous density with respect to the Lebesgue measure, the probability of taking any particular value is 0. In particular,

$$Pr(\gamma_i = 0 | \mathbf{N}_{..i} \neq 0) = 0,$$

and thus $Pr(\gamma_j \neq 0 | \mathbf{N}_{\cdot,j} \neq 0) = 1$. This proves the second equation and finishes the proof.

Lemma 9. The function $P_j(w) \triangleq (\sum_{i=0}^{r_c+s-1} a_{i+1} w^i)/(w^s + \sum_{i=0}^{s-1} a_{i+r_c+s+1} w^i)$ is a well-defined polynomial. In fact, we have $P_j(w) = \sum_{k=0}^{r_c-1} u_{k+1} w^k$, where $u_k \triangleq \sum_{\ell=1}^{d_c} \mathbf{f}_{\ell}[\mathbf{Y}_{rj}\mathbf{1}_{P}]_{k+(\ell-1)r_c}$.

Proof. Let $\bar{\mathbf{y}}_j \triangleq \mathbf{Y}_{rj} \mathbf{1}_P$. Let i_1, i_2, \dots, i_s denote be the indices of adversarial/Byzantine nodes in the jth group. Construct polynomials

$$P(w) = \prod_{k=1}^{s} (w - w_{i_k}) \triangleq w^s + \sum_{k=0}^{s-1} \theta_k w^k$$

and for u_k defined in the statement of the lemma,

$$Q(w) = \sum_{k=0}^{r_c - 1} u_{k+1} w^k.$$

Let

$$R(w) = P(w)Q(w) \triangleq \sum_{k=0}^{r_c+s-1} \beta_k w^k.$$

Recall that $\mathbf{r}_{j,c} = \mathbf{f} \mathbf{R}_j$. When $(j-1)r + k = i_\ell$ for some ℓ , by definition, we have $P(w_{(j-1)r+k}) = 0$ and thus

$$P(w_{(j-1)r+k}) \left[\mathbf{r}_{j,c} \right]_k = 0 = P(w_{(j-1)r+k}) Q(w_{(j-1)r+k}).$$

When $(j-1)r + k \neq i_{\ell}$ for any ℓ , by definition, the (j-1)r + kth node, or the kth node in the jth group, is not adversarial/Byzantine. By definition,

$$\begin{aligned} [\mathbf{r}_{j,c}]_k = & [\mathbf{f}\mathbf{R}_j]_k = \mathbf{f}[\mathbf{R}_j]_{\cdot,k} = \mathbf{f}\mathbf{z}_{(j-1)r+k} \\ = & \mathbf{f}\mathbf{W}_{(j-1)r+k}\mathbf{Y}_{(j-1)r+k}\mathbf{1}_P = \mathbf{f}\mathbf{W}_{(j-1)r+k}\mathbf{Y}_{rj}\mathbf{1}_P. \end{aligned}$$

This can be written as

$$\mathbf{fW}_{(j-1)r+k}\bar{\mathbf{y}}_{j} = \mathbf{fI}_{d_{c}} \otimes [1, w_{(j-1)r+k}, w_{(j-1)r+k}^{2}, \dots, w_{(j-1)r+k}^{r_{c}-1}]\bar{\mathbf{y}}_{j}.$$

This in turn equals

$$\begin{split} \sum_{p=1}^{d_c} \mathbf{f}_p \sum_{\ell=0}^{r_c-1} w_{(j-1)r+k}^{\ell} [\bar{\mathbf{y}}_j]_{\ell+1+(p-1)r_c} &= \sum_{\ell=0}^{r_c-1} \sum_{p=1}^{d_c} \mathbf{f}_p [\bar{\mathbf{y}}_j]_{\ell+1+(p-1)r_c} w_{(j-1)r+k}^{\ell} \\ &= \sum_{\ell=0}^{r_c-1} u_{\ell+1} w_{(j-1)r+k}^{\ell} = Q(w_{(j-1)r+k}). \end{split}$$

That is, $[\mathbf{r}_{j,c}]_k = Q(w_{(j-1)r+k})$, which implies

$$P(w_{(j-1)r+k})[\mathbf{r}_{j,c}]_k = P(w_{(j-1)r+k})Q(w_{(j-1)r+k}).$$

Noting that P(w)Q(w) = R(w), we have

$$P(w_{(i-1)r+k})[\mathbf{r}_{i,c}]_k = R(w_{(i-1)r+k})$$
(A.1)

for any k.

This is a linear system for the vector $\mathbf{b} \triangleq [\beta_0, \beta_1, \dots, \beta_{r_c+s-1}, \theta_0, \theta_1, \dots, \theta_{s-1}]^T$. Rewriting the system in a compact way, we have

$$\begin{bmatrix} \hat{\mathbf{W}}_{j,r_c+s-1}, & -\hat{\mathbf{W}}_{j,s-1} \odot \left(\mathbf{y} \mathbf{1}_s^T\right) \end{bmatrix} \mathbf{b} = \mathbf{r}_{j,c} \odot \begin{bmatrix} \hat{\mathbf{W}}_{j,s} \end{bmatrix}_{\cdot,s}.$$

There are now two cases to consider.

(i) Solving the linear system leads to $\mathbf{a} = \mathbf{b}$. Then by construction of $P_i(w)$, we have

$$P_j(w) = (\sum_{i=0}^{r_c+s-1} a_{i+1} w^i) / (w^s + \sum_{i=0}^{s-1} a_{i+r_c+s+1} w^i) = R(w) / P(w) = Q(w) = \sum_{k=0}^{r_c-1} u_{k+1} w^k.$$

The second equality follows by plugging in the solution $\mathbf{a} = \mathbf{b}$ into the definition of both the numerator and the denominator of P_j . Then we see that the numerator reduces to $\sum_{k=0}^{r_c+s-1} \beta_k w^k = R(w)$, while the denominator reduces to $w^s + \sum_{k=0}^{s-1} \theta_k w^k = P(w)$. The third equality follows due to the definition of R = PQ, while the last equality holds due to the definition of Q.

(ii) Solving the linear system gives another solution $\tilde{\mathbf{b}} = [\tilde{\beta}_0, \tilde{\beta}_1, \dots, \tilde{\beta}_{r_c+s-1}, \tilde{\theta}_0, \tilde{\theta}_1, \dots, \tilde{\theta}_{s-1}]^T$. Construct polynomials $\tilde{P}(w) = w^s + \sum_{k=0}^{s-1} \tilde{\theta}_k w^k$ and $\tilde{R}(w) = \sum_{k=0}^{r_c+s-1} \beta_k w^k$. Since $\tilde{\mathbf{b}}$ is a solution to the original linear system, we must have

$$\tilde{P}(w_{(r-1)j+k}) [\mathbf{r}_{j,c}]_k = \tilde{R}(w_{(r-1)j+k}).$$
 (A.2)

We can combine this with (A.1). If $P(w_{(r-1)j+k})$ and $\tilde{P}(w_{(r-1)j+k})$ are not zero, then we have

$$\tilde{R}(w_{(r-1)j+k})/\tilde{P}(w_{(r-1)j+k}) = \left[\mathbf{r}_{j,c}\right]_k = R(w_{(r-1)j+k})/P(w_{(r-1)j+k})$$

which implies

$$\tilde{R}(w_{(r-1)j+k})P(w_{(r-1)j+k}) = R(w_{(r-1)j+k})\tilde{P}(w_{(r-1)j+k}). \tag{A.3}$$

If $P(w_{(r-1)j+k})=0$, then by (A.1), $R(w_{(r-1)j+k})=0$, and hence (A.3) still holds. If $\tilde{P}(w_{(r-1)j+k})=0$, then similarly by (A.2), $\tilde{R}(w_{(r-1)j+k})=0$, and hence (A.3) also holds. Therefore, (A.3) holds for any k. For fixed j, the index k can take in total $r=r_c+2s$ values, and the degrees of both $P(w)\tilde{R}(w)$ and $\tilde{P}(w)R(w)$ are r_c+2s-1 . Thus, we must have for all w

$$\tilde{R}(w)P(w) = R(w)\tilde{P}(w)$$

and hence

$$P_j(w) = \tilde{R}(w)/\tilde{P}(w) = R(w)/P(w) = Q(w) = \sum_{k=0}^{r_c-1} u_{k+1} w^k.$$

Thus $P_j(w) = \sum_{k=0}^{r_c-1} u_{k+1} w^k$ is a well-defined polynomial, finishing the proof.

Now we are ready to prove the lemma, by a calculation very similar to the one we have done earlier in the proof of Lemma 9. By definition,

$$[\mathbf{r}_{j,c}]_k = [\mathbf{f}\mathbf{R}_j]_k = \mathbf{f}[\mathbf{R}_j]_{\cdot,k} = \mathbf{f}(\mathbf{z}_{(j-1)r+k} + \mathbf{n}_j)$$

= $\mathbf{f}\mathbf{W}_{(j-1)r+k}\mathbf{Y}_{(j-1)r+k}\mathbf{1}_P + \mathbf{f}\mathbf{n}_j = \mathbf{f}\mathbf{W}_{(j-1)r+k}\mathbf{Y}_{rj}\mathbf{1}_P + \mathbf{f}\mathbf{n}_j.$

This can be written as

$$\mathbf{fW}_{(j-1)r+k}\bar{\mathbf{y}}_j + \mathbf{fn}_j = \mathbf{fI}_{d_c} \otimes [1, w_{(j-1)r+k}, w_{(j-1)r+k}^2, \dots, w_{(j-1)r+k}^{r_c-1}]\bar{\mathbf{y}}_j + \mathbf{fn}_j.$$

This equals

$$\begin{split} \sum_{p=1}^{d_c} \mathbf{f}_p \sum_{\ell=0}^{r_c-1} w_{(j-1)r+k}^{\ell} [\bar{\mathbf{y}}_j]_{\ell+1+(p-1)r_c} + \mathbf{f} \mathbf{n}_j &= \sum_{\ell=0}^{r_c-1} \sum_{p=1}^{d_c} \mathbf{f}_p [\bar{\mathbf{y}}_j]_{\ell+1+(p-1)r_c} w_{(j-1)r+k}^{\ell} + \mathbf{f} \mathbf{n}_j \\ &= \sum_{\ell=0}^{r_c-1} u_{\ell+1} w_{(j-1)r+k}^{\ell} = P_j(w_{(j-1)r+k}) + \mathbf{f} \mathbf{n}_j. \end{split}$$

Thus, $[\mathbf{r}_{j,c}]_k = P_j(w_{(j-1)r+k}) + \mathbf{f}\mathbf{n}_j$. By Lemma 8, with probability equal to unity, $\mathbf{f}\mathbf{n}_j = \gamma_j = 0$ if and only if $\|\mathbf{n}_j\| = 0$. In other words, with probability equal to unity, $[\mathbf{r}_{j,c}]_k \neq P_j(w_{(j-1)r+k})$ if and only if $\|\mathbf{n}_j\| \neq 0$, which demonstrates the correctness of Lemma 3.

A.4 Proof of Lemma 4

Proof. The *j*th node needs to to compute and send to the PS

$$\mathbf{z}_i = \mathbf{W}_i \mathbf{Y}_i \mathbf{1}_P$$
.

Due to the assignment matrix **A**, all nodes in group j compute the same \mathbf{Y}_j , so $\mathbf{Y}_{(j-1)r+k} = \mathbf{Y}_{jr}$, for $k \in \{1, 2, ..., r\}$. Let us partition $\mathbf{Y}_{jr}\mathbf{1}_P$ into d/r vectors of size $r \times 1$, i.e.,

$$\mathbf{Y}_{jr}\mathbf{1}_{P} riangleq egin{bmatrix} \mathbf{Y}_{jr,1} \ \mathbf{Y}_{jr,2} \ \dots \ \mathbf{Y}_{jr,d/r} \end{bmatrix}.$$

Then we have

$$\begin{split} \mathbf{r}_{(j-1)r+k} = & \mathbf{W}_{(j-1)r+k} \mathbf{Y}_{jr} \mathbf{1}_{P} = \mathbf{I}_{d_{c}} \otimes [1, w_{(j-1)r+1}, w_{(j-1)r+2}^{2}, \dots, w_{jr}^{r_{c}-1}] \begin{bmatrix} \mathbf{Y}_{jr,1} \\ \mathbf{Y}_{jr,2} \\ \dots \\ \mathbf{Y}_{jr,d/r} \end{bmatrix} \\ = \begin{bmatrix} [1, w_{(j-1)r+1}, w_{(j-1)r+2}^{2}, \dots, w_{jr}^{r_{c}-1}] \mathbf{Y}_{jr,1} \\ [1, w_{(j-1)r+1}, w_{(j-1)r+2}^{2}, \dots, w_{jr}^{r_{c}-1}] \mathbf{Y}_{jr,2} \\ \dots \\ [1, w_{(j-1)r+1}, w_{(j-1)r+2}^{2}, \dots, w_{jr}^{r_{c}-1}] \mathbf{Y}_{jr,d/r} \end{bmatrix}. \end{split}$$

Therefore,

$$\left[\mathbf{z}_{(j-1)r+1},\mathbf{z}_{(j-1)r+2},\ldots,\mathbf{z}_{jr}
ight] = egin{bmatrix} \left[\hat{\mathbf{W}}_{j,r_c-1}\mathbf{Y}_{jr,1}
ight]^T \ \hat{\mathbf{W}}_{j,r_c-1}\mathbf{Y}_{jr,2}
ight]^T \ & \ldots \ \left[\hat{\mathbf{W}}_{j,r_c-1}\mathbf{Y}_{jr,d/r}
ight]^T \end{bmatrix}.$$

By definiton, we have

$$\begin{split} \mathbf{R}_j &= \left[\mathbf{z}_{(j-1)r+1}, \mathbf{z}_{(j-1)r+2}, \dots, \mathbf{z}_{jr}\right] + \left[\mathbf{n}_{(j-1)r+1}, \mathbf{n}_{(j-1)r+2}, \dots, \mathbf{n}_{jr}\right] \\ &= \begin{bmatrix} \left[\hat{\mathbf{W}}_{j,r_c-1} \mathbf{Y}_{jr,1}\right]^T \\ \left[\hat{\mathbf{W}}_{j,r_c-1} \mathbf{Y}_{jr,2}\right]^T \\ & \dots \\ \left[\hat{\mathbf{W}}_{j,r_c-1} \mathbf{Y}_{jr,d/r}\right]^T \end{bmatrix} + \left[\mathbf{n}_{(j-1)r+1}, \mathbf{n}_{(j-1)r+2}, \dots, \mathbf{n}_{jr}\right]. \end{split}$$

According to Lemma 3 and its assumptions, with probability equal to unity, the index set V contains all adversarial node indices and thus U contains all the non-adversarial node indices. Thus, if $k \in U$, then $\mathbf{n}_{(j-1)r+k} = \mathbf{0}$, and the kth column of \mathbf{R}_j only contains the first term in the above equation. More precisely, we have

$$\begin{split} \left[\mathbf{R}_{j}\right]_{.,U} &= \left[\mathbf{z}_{(j-1)r+1}, \mathbf{z}_{(j-1)r+2}, \ldots, \mathbf{z}_{jr}\right]_{.,U} = \begin{bmatrix} \left[\hat{\mathbf{W}}_{j,r_{c}-1}\mathbf{Y}_{jr,1}\right]^{T} \\ \left[\hat{\mathbf{W}}_{j,r_{c}-1}\mathbf{Y}_{jr,2}\right]^{T} \\ \ldots \\ \left[\hat{\mathbf{W}}_{j,r_{c}-1}\mathbf{Y}_{jr,d/r}\right]^{T} \end{bmatrix}_{.,U} \\ &= \begin{bmatrix} \mathbf{Y}_{jr,1}^{T} \left[\hat{\mathbf{W}}_{j,r_{c}-1}\right]_{.,U}^{T} \\ \mathbf{Y}_{jr,2}^{T} \left[\hat{\mathbf{W}}_{j,r_{c}-1}\right]_{.,U}^{T} \\ \ldots \\ \mathbf{Y}_{jr,d/r}^{T} \left[\hat{\mathbf{W}}_{j,r_{c}-1}\right]_{.U}^{T} \end{bmatrix} = \begin{bmatrix} \mathbf{Y}_{jr,1}^{T} \\ \mathbf{Y}_{jr,2}^{T} \\ \ldots \\ \mathbf{Y}_{jr,d/r}^{T} \end{bmatrix} \begin{bmatrix} \hat{\mathbf{W}}_{j,r_{c}-1} \end{bmatrix}_{.,U}^{T} . \end{split}$$

Note that and r_c rows of $\left[\hat{\mathbf{W}}_{j,r_c-1}\right]^T$ is $\left[\hat{\mathbf{W}}_{j,r_c-1}\right]_{\cdot,U}^T$ must be invertible. We can then multiply each side by the inverse of $\left[\hat{\mathbf{W}}_{j,r_c-1}\right]_{\cdot,U}^T$ yielding

$$\left[\mathbf{R}_{j}
ight]_{.,U}\left[\hat{\mathbf{W}}_{j,r_{c}-1}^{-T}
ight]_{.,U}^{-1} = egin{bmatrix} \mathbf{Y}_{jr,1}^{T} \ \mathbf{Y}_{jr,2}^{T} \ & \ddots \ \mathbf{Y}_{jr,d/r}^{T} \end{bmatrix}.$$

Vectorizing it gives the desired gradients, we obtain

$$vec\left(\left[\mathbf{R}_{j}\right]_{\cdot,U}\left[\hat{\mathbf{W}}_{j,r_{c}-1}^{T}\right]_{\cdot,U}^{-1}\right) = \begin{bmatrix} \mathbf{Y}_{jr,1} \\ \mathbf{Y}_{jr,2} \\ \cdots \\ \mathbf{Y}_{jr,d/r} \end{bmatrix} = \mathbf{Y}_{jr}\mathbf{1}_{P}.$$

A.5 Proof of Theorem 5

Proof. Recall that Lemma 3 implies that with probability equal to unity, $V = \phi(\mathbf{R}_j, j) = \{i : \|\mathbf{n}_{j(r-1)+i}\|_0 \neq 0\}$. Since $|\{j : \|\mathbf{n}_j\|_0 \neq 0\}| \leq s$, we must have $|V| \leq s$. Therefore, $|U| = |\{1, 2, ..., r\} - V| \geq r - s$, and U only contains the non-adversarial nodes with probability equal to unity. By Lemma 4, we have $\mathbf{u}_j = \sum_{k=(j-1)r+1}^{jr} \mathbf{g}_k$ for j = 1, 2, ..., P/r. Therefore,

$$\sum_{j=1}^{P/r} \mathbf{u}_j = \sum_{j=1}^{P/r} \sum_{k=(j-1)r+1}^{jr} \mathbf{g}_k = \sum_{j=1}^{P} \mathbf{g}_j = \mathbf{G} \mathbf{1}_P.$$

This shows we correctly recover the sum of the gradient updates, while tolerating s Byzantine nodes and ensuring communication compression ratio r_c .

Now let us consider the encoder and decoder complexity. For the encoder, first $\mathbf{Y}_j\mathbf{1}_P$ takes $\mathcal{O}(dr)$ flops, i.e., elementary addition and multiplication operations. Second, directly computing $\mathbf{W}_j(\mathbf{Y}_j\mathbf{1}_P)$ takes $\mathcal{O}(d_cd)$ flops. However, by definition $\mathbf{W}_j = \mathbf{I}_{d_c} \otimes [1, w_j, w_j^2, \dots, w_j^{r_c-1}]$ is a sparse matrix with r_c nonzeros per row. Therefore, using sparse matrix computation, it only takes $\mathcal{O}(d_cr_c) = \mathcal{O}(d)$ computations. Thus, the encoder function needs in total $\mathcal{O}(dr) + \mathcal{O}(d) = \mathcal{O}(dr)$ computations. For the decoder, obtaining the adversarial node indices needs $\mathcal{O}(d_cr)$ for computing $\mathbf{r}_{j,c} = \mathbf{f}\mathbf{R}_j$. Solving the linear system takes $\mathcal{O}(r^3)$. Computing the polynomial needs

$$\mathcal{O}\left(\frac{r_c+s-1}{s}(r_c+s-1+s)\right) = \mathcal{O}\left(r_c^2/s+r_c+s\right).$$

Evaluating the polynomial takes $\mathcal{O}(r(r_c-1)) = \mathcal{O}(rr_c)$. Computing $\left[\hat{W}_{j,r_c-1}^T\right]_{U,\cdot}^{-1}$ needs $\mathcal{O}(r_c^3)$, and computing $\left[\mathbf{R}_j\right]_{\cdot,U}\left[\hat{W}_{j,r_c-1}^T\right]_{U}^{-1}$ needs $\mathcal{O}(d_cr_c^3)$. Therefore, in total we need

$$\mathcal{O}(d_c r) + \mathcal{O}(r^3) + \mathcal{O}(r_c^2/s + r_c + s) + \mathcal{O}(r r_c) + \mathcal{O}(r_c^3) + \mathcal{O}(d_c r_c^2) = \mathcal{O}(d_c r + r^3 + d_c r_c^2).$$

There are in total P/r iterations, so we have in total

$$P/r \cdot \mathcal{O}(d_c r + r^3 + d_c r_c^2) = \mathcal{O}(Pr^2 + Pd_c + Pd_c r_c^2/r)$$

flops. The final sum of all \mathbf{u}_i takes $\mathcal{O}(P/r \cdot d) = \mathcal{O}(Pd/r)$. Thus, in total we have

$$\mathcal{O}(Pd_c + Pr^2 + Pd_c r_c^2/r + Pdr_c/r) = \mathcal{O}(Pd/r_c + Pr^2 + Pdr_c/r).$$

Suppose $d \gg P$, i.e., $d = \blacksquare(P^2)$. Note that the redundancy ratio cannot be larger than P, we know $r \leq P$ and thus, $r^2 \leq P^2 = \blacksquare(d)$. This implies that

$$\mathcal{O}(Pd_c + Pr^2 + Pd_c r_c^2/r + Pdr_c/r) = \mathcal{O}(Pd/r_c + Pr^2 + Pdr_c/r) = \mathcal{O}(Pd(1 + \frac{1}{r_c} + \frac{r_c}{r}))$$

Thus, we have shown that the complexity of encoder and function is linear in the dimension of the gradient and the redundancy ratio, while that of the decoder is linear in the dimension of the gradient and the number of computing nodes P.

B Equivalence of the Byzantine recovery to sparse recovery in Section 3.4

Here we explain how the problem of deigning a regular mechanism is equivalent to a sparse recover problem. We consider the setting, where we want to recover a d-dimensional vector g from $m := rd_c$ -dimensional observations R = Zg + n, where n is $k := sd_c$ -sparse. First we argue that there are many design matrices Z

that allow this. As we saw, the requirement on Z is that when $Zv \in B_{2s,r}$, then v=0. Suppose $w=Zv \in B_{2s,r}$ and let S be the set of size at most k of the nonzero coordinates of w. Letting $Z'=Z_{S^c}$, be the $(m-|S|)\times d$ matrix formed by the rows of Z outside of S, we have that Z'v=0. If $m-|S|\geq d$ and Z' has full rank d, then this implies v=0 and we are done. As $|S|\leq 2k$, it is enough to ensure that each $(m-2k)\times d$ submatrix formed by the rows of Z has rank r. When $m-2k\geq r$, this holds with probability one when—for instance—the entries of Z are sampled iid from a distribution with a density that is absolutely continuous with respect to the Lebesgue measure. The reason is that the set of rank-deficient matrices is a set of zero Lebesgue measure in the space of all matrices [33].

Thus, we have such a matrix Z and the observation R = Zg + n, where n is k-sparse, and the goal is to find the unique vector g such that R = Zg + n. It is possible to solve this problem by enumerating all subsets S of size at most k to find the unique subset for which $R_{S^c} \in span(Z_{S^c}, \cdot)$, or equivalently $P_SR_{S^c} = 0$, where P_S is the projection into the orthocomplement of the column span of the matrix Z_{S^c} ,. This is a combinatorial algorithm, which requires a search over $\binom{m}{k}$ subsets, and thus illustrates the challenges of this problem.

In fact, multiplying R=Zg+n with an orthogonal complement Z^{\perp} such that $Z^{\perp}Z=0_{m-d,d}$, we see that it is sufficient to be able to find the unique k-sparse n such that $y=Z^{\perp}n$, where $y:=Z^{\perp}R$. Moreover, this is also necessary, because uniqueness means that $y=Z^{\perp}n=Z^{\perp}n'$, or also $Z^{\perp}(n'-n'')=0$ implies n-n'=0, or equivalently that $Ker(Z^{\perp})\cap B_{2s,r}=\{0\}$. Since $Ker(Z^{\perp})=Im(Z)$, this is equivalent to the previous claim. In conclusion, our question is exactly equivalent to a sparse recovery problem, finishing the argument.

C Experimental Details

Additional experimental details are discussed here.

Experimental setups. All experiments were conducted on a cluster of 50 machines. Each machine is equipped with 20 Intel Xeon E5-2660 2.6 GHz cores, 160 GB RAM, and 200GB disk with Ubuntu 18.04 LTS as the OS. All code was implemented in Python 3.8. The entire experiments took several months, including debugging and evaluation time. Note that this is mostly because the defense approach BULYAN is slow. Evaluating SOLONalone can be much faster. In addition, SOLONwas built in Python for demonstration purposes. Code optimization with addition tools (such as Cython) can give extra speedups.

Hyper-parameters. We evaluate SOLON, BULYAN, DRACO, and SIGNUM using the datasets and models in Table 1. We add vanilla SGD without any Byzantine adversary as the gold standard for accuracy. Our cluster consists of one parameter server (PS) and 100 compute nodes, hosted on 50 real c220g5 machines. SOLON and DRACO partition the compute nodes evenly into 5 groups. The training batch size for SOLON and DRACO is 120 per group, and equivalently six per compute node for other baselines. We fix the compression ratio r_c to 10, except in the experiment where we evaluate the effect of compression ratio. For DRACO, we only test its repetition code scheme, since the cyclic code scheme has a slightly slower performance [12]. We calculate the redundancy ratio by r = 2s + 1 for DRACO. To compare with the best possible performance of DRACO, we set its r = 11 such that it only uses 55 compute nodes to reduce communication overhead in the end-to-end performance test. These methods are trained for 3,000 iterations and evaluated on the test set every 25 steps. The learning rate is set to 0.1.

Under the constant attack, however, we found that SIGNUM may diverge. We therefore decay the learning rate as $5 \cdot 10^{-5} \cdot 0.95^{\lfloor t/10 \rfloor}$ for SIGNUM to get a more stable accuracy curve in Figure 2(b), where t is the number of iterations. We also observe that BULYAN does not converge under the ALIE attack, matching the observation in [42]. We therefore lower the learning rate to $0.002 \cdot 0.95^{\lfloor t/10 \rfloor}$ in order to enable BULYAN to converge to a lower accuracy in Figure 2(c).

For language model task using LSTM over Wikitext-2 dataset, we observe that BULYAN and SIGNUM do not converge very well under small batches. We then decide not to keep the linearity of batch size (batch size linearity is mentioned in [53]) among SOLON and these two baselines. As a result, the batch size setting is

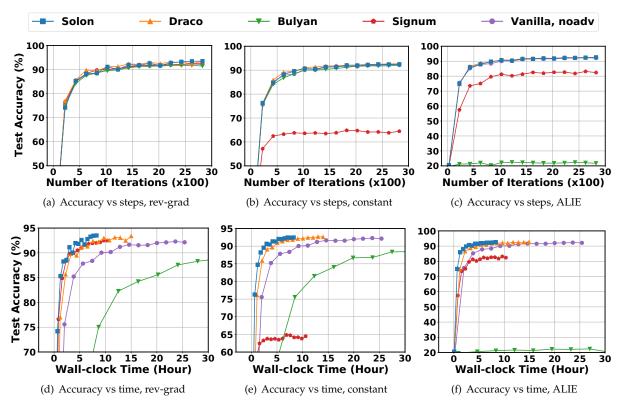


Figure 6: End to end convergence performance of SOLON and other baselines on VGG13-BN and SVHN.

b=3 for Vanilla SGD with LSTM and b=60 for others. The learning rate is set as lr=40 during SOLON, DRACO, Vanilla SGD, and lr=20 for BULYAN and SIGNUM. We use learning rate warm-up for the first 800 iterations of SOLON, DRACO and Vanilla SGD, and during the first 400 iterations for the rest of two. Since we observe in previous experiments that BULYAN and SIGNUM fail in ALIE and constant attacks respectively, we only show their performance under reverse-gradient attack.

D Additional Empirical Results

Now we give additional empirical findings. The goal is to (i) verify if SOLON's performance gain is valid in wider applications, (ii) study how the number of Byzantine attacks s as well as the compression ratio r_c may affect the performance of SOLON, and (iii) understand the computational cost of SOLON's decoder.

End to end convergence performance, ctd. To verify if SOLON is substantially more robust and efficient in wider applications, we conducted evaluations for training an additional model, VGG13 on SVHN. Figure 6 shows the end to end performance of SOLONand other baselines under a few different attacks. Overall, we observe similar trends seen for other models in the main paper. Generally, SOLON converges to the same accuracy level of vanilla SGD under no Byzantine attack, while providing much faster runtime performance than all baselines. BULYAN and SIGNUM fail by losing around 60% and 30% accuracy under ALIE and constant attack in the experiment of VGG13+SVHN. However, we notice two slight differences. First, the advantage in runtime performance of SOLON in Figure 6 seems to be not as remarkable as it is in RN18 (Figure 2). This is because SVHN dataset is an easier task and the model accuracy rises faster than ResNet18+CIFAR10. It then makes the baseline performances look better. However, if there are harder tasks where the accuracy climbs slower, the advantage of SOLON will be clearer. Second, BULYAN and

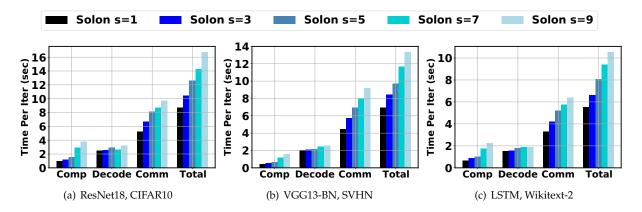


Figure 7: Time breakdown per iteration of SOLON, varying s with fixed $r_c = 10$ over three models+datasets. The redundancy ratio is set as $r = 2s + r_c$, and thus increases as s increases. It is easy to see that all costs increase linearly as the number of adversaries s increases.

SIGNUM perform worse than SOLON both in final accuracy and runtime in the language model task of LSTM+Wikitext-2. We think it's because this task is more sensitive to gradient changes, such that the exact gradient recovery schemes like SOLON have better performance than approximated ones.

The influence of the number of adversaries. We now evaluate the effects of the number s of adversaries on the runtime of SOLON, as shown in Figure 7. We observe that the computation time, communication time and decoding time of SOLON increase roughly linearly as the number of adversaries s increases. This is reasonable, because the minimum redundancy ratio r increases with the number of adversaries s, when r_c is fixed. This leads to an increase in the total number of workers and batch sizes, i.e., the communication and computation overhead. This result shows that the cost of SOLON increases linearly as s increases, and verifies that SOLON is scalable to distributed training.

The effects of the compression ratio, ctd. In the main text, we showed the effects of the compression ratio r_c when s and number of nodes P are fixed for ResNet-18. The remaining results for VGG13 and LSTM are shown in Figure 8. Overall, the total time decreases as r_c increases, showing that SOLON is efficient in reducing communication time and can be applied to large clusters. But there are some subtleties. First, the communication time decreases as r_c increases, because the size of compressed gradients decreases. However,

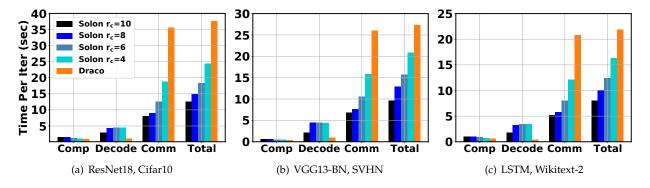


Figure 8: Time breakdown per iteration of SOLON over three models+datasets, varying r_c with fixed s = 5. The redundancy ratio is calculated as $r = 2s + r_c$, and thus increases when r_c increases from 2 to 10.

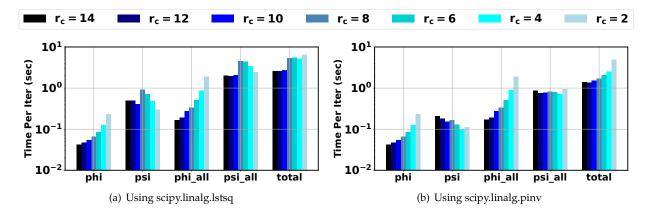


Figure 9: Decoder time breakdown per iteration of SOLON over ResNet-18+CIFAR-10, varying r_c with fixed s=5, in log scale. (a) Using linear equation solver to build ψ . (b) Using pseudo-inverse to build ψ . "phi" and "psi" refer to the single execution time for function ϕ and ψ . "phi_all" and "psi_all" refer to the execution time of the designated functions for all groups in the whole cluster. "total" means the complete decoding time per iteration.

when r_c becomes larger, the additional benefit of communication cost becomes smaller. This is because the increase of the redundancy ratio r adds some overhead. Also, the overhead in communication also limits the best possible communication results achieved. Next, the computation time increases linearly when r_c increases from two to 10. This is also because the number of groups gradually decreases as r increases, which introduces larger batch sizes for each group in order to maintain total equivalent batch sizes. This overhead is common across all three tasks.

In addition, we push the analysis on the decoding time one step further, where the breakdown results are shown in Figure 9(a). To test the decoder time breakdown, we fix the maximum number of threads used by pytorch by setting MKL_NUM_THREADS = 10 instead of 20 in the previous end to end tests to avoid all possible computing resource conflict on a single machine. On the first glance, the total decoding time does not seem to have a clear pattern when r_c increases. However, we notice that the time for $\phi(\cdot)$ increases almost linearly as d_c increases (by decreasing r_c). This is reasonable because the major overhead for ϕ is computing $\mathbf{r}_{j,c} = \mathbf{f}\mathbf{R}_j$, of which the computation complexity is $O(P/r \cdot r \cdot d_c) = O(Pd_c) = O(Pd/r_c)$ as discussed in Section 3, Algorithm 1 and Appendix Section C. On the other hand, the time for ψ seems to be non-monotonic, but the major overhead is to solve the linear system $\left[\hat{\mathbf{W}}_{j,r_c+s-1}, -\hat{\mathbf{W}}_{j,s-1}\odot\left(\mathbf{r}_{j,c}^T\mathbf{1}_s^T\right)\right]\mathbf{a} = \mathbf{r}_{j,c}\odot\left[\hat{\mathbf{W}}_{j,s}\right]$ whose computation complexity is roughly $\mathcal{O}(Pr^2 + Pdr_c/r)$. We later realize that the non-monotonicity is caused by the linear equation solver "scipy.linalg.lstsq". When we altered the solver using "scipy.linalg.pinv" presented in Figure 9(b), we observe that the time for ψ is decreasing monotonically as r_c decreases, which matches the theoretical analysis. We then argue that the implementation of the linear solver would determine the actual runtime performance of the decoder. Thus, we end the discussion here at the breakdown level of python functions, since the efficient design, implementation and analysis of the linear solvers are beyond the scope of this work.

E Potential Limitation of SOLON.

Discussion. To conclude our evaluations, SOLON greatly reduces communication cost and is scalable to large clusters, but its parameters should be chosen carefully for different cluster resources and tasks. An interesting question is when to use SOLON instead of other methods. The experiments and discussions already reveal a partial answer. If there are strong attacks in term of the attack ratio and attack type and limited network bandwidth, but higher accuracy is demanded, SOLON is preferred. On the contrary, if the

attacks are expected to be weak, and if quick results are needed with less precision, algorithms which use more approximations—such as SIGNUM and its further variations—can be chosen. In addition, SOLON requires $r \geq 2s + r_c$ and r dividing P, which may require some tuning on the number of machines used. Furthermore, r_c cannot be too large. Extremely large r_c wastes computing resources, and may cause numerical issues in decoding (e.g., as we observed when $r_c > 14$ and precision is limited). As future work, we will consider developing a set of rules to pick the best Byzantine-resilient algorithm given a scenario, and developing SOLON variations for asynchronous and decentralized training.